


8-2016

Role of river bathymetry in hydraulic modeling of river channels

Sayan Dey
Purdue University

Follow this and additional works at: https://docs.lib.purdue.edu/open_access_theses

 Part of the [Civil Engineering Commons](#), [Hydrology Commons](#), and the [Water Resource Management Commons](#)

Recommended Citation

Dey, Sayan, "Role of river bathymetry in hydraulic modeling of river channels" (2016). *Open Access Theses*. 940.
https://docs.lib.purdue.edu/open_access_theses/940

This document has been made available through Purdue e-Pubs, a service of the Purdue University Libraries. Please contact epubs@purdue.edu for additional information.

**PURDUE UNIVERSITY
GRADUATE SCHOOL
Thesis/Dissertation Acceptance**

This is to certify that the thesis/dissertation prepared

By SAYAN DEY

Entitled

ROLE OF RIVER BATHYMETRY IN HYDRAULIC MODELING OF RIVER CHANNELS

For the degree of Master of Science in Civil Engineering

Is approved by the final examining committee:

VENKATESH M. MERWADE

Chair

DENNIS A. LYN

MARTY D. FRISBEE

To the best of my knowledge and as understood by the student in the Thesis/Dissertation Agreement, Publication Delay, and Certification Disclaimer (Graduate School Form 32), this thesis/dissertation adheres to the provisions of Purdue University's "Policy of Integrity in Research" and the use of copyright material.

Approved by Major Professor(s): VENKATESH M. MERWADE

Approved by: DULCY M. ABRAHAM

Head of the Departmental Graduate Program

7/25/2016

Date

ROLE OF RIVER BATHYMETRY IN HYDRAULIC MODELING OF RIVER
CHANNELS

A Thesis

Submitted to the Faculty

of

Purdue University

by

Sayan Dey

In Partial Fulfillment of the

Requirements for the Degree

of

Master of Science in Civil Engineering

August 2016

Purdue University

West Lafayette, Indiana

For my parents

ACKNOWLEDGEMENTS

First and foremost, I would like to express my gratitude to my advisor, Prof. Venkatesh Merwade, for his constant support and guidance during my research. I would also like to thank Prof. Dennis Lyn and Prof. Marty Frisbee for serving on my committee.

Part of the dataset used in this study was provided by USGS Indiana Water Data Center, North Carolina Floodplain Mapping Program (NCFMP) and Fort Bend County, Texas, without which this study would not have been possible.

Finally, I am thankful to my friend and colleague, Siddharth Saksena, for his insights and feedback that helped in improving the study.

TABLE OF CONTENTS

| | Page |
|---|------|
| LIST OF TABLES..... | vi |
| LIST OF FIGURES..... | vii |
| LIST OF ABBREVIATIONS..... | ix |
| ABSTRACT..... | x |
| CHAPTER 1. INTRODUCTION..... | 1 |
| 1.1 Background and Study Objective..... | 1 |
| 1.2 Approach..... | 3 |
| 1.3 Thesis Organization..... | 4 |
| CHAPTER 2. LITERATURE REVIEW..... | 5 |
| 2.1 Introduction..... | 5 |
| 2.2 Methods of acquiring bathymetry data..... | 5 |
| 2.2.1 Field Survey Techniques..... | 5 |
| 2.2.2 Remote Sensing..... | 7 |
| 2.3 Conceptual models to estimate bathymetry..... | 9 |
| 2.4 Summary..... | 11 |
| CHAPTER 3. STUDY AREA AND DATA..... | 12 |
| 3.1 Introduction..... | 12 |
| 3.2 Study Reaches..... | 13 |
| 3.2.1 Strouds Creek..... | 13 |
| 3.2.2 Tippecanoe River..... | 14 |
| 3.2.3 St. Joseph River..... | 15 |
| 3.2.4 East Fork White River..... | 16 |

| | Page |
|--|------|
| 3.2.5 Brazos River..... | 17 |
| 3.3 Flow Data..... | 18 |
| 3.4 LIDAR and Bathymetric Data..... | 21 |
| CHAPTER 4. METHODOLOGY..... | 23 |
| 4.1 Introduction..... | 23 |
| 4.2 Description of Bathymetric Models..... | 24 |
| 4.2.1 Linear Interpolation (Linear1 and Linear2)..... | 25 |
| 4.2.2 RCMM (RCMM1 and RCMM2)..... | 26 |
| 4.2.3 LIDAR..... | 28 |
| 4.3 Bathymetry Integration..... | 29 |
| 4.4 Hydraulic Modeling..... | 29 |
| 4.5 Comparison of Bathymetric Configurations..... | 31 |
| CHAPTER 5. RESULTS AND DISCUSSION..... | 33 |
| 5.1 Introduction..... | 33 |
| 5.2 Comparison of DEM and Estimated Cross-sections..... | 33 |
| 5.3 Comparison of Inundation Mapping..... | 37 |
| 5.4 Comparison of Flow Areas at Cross-section..... | 49 |
| 5.5 Comparison of Velocity and Shear Estimates..... | 51 |
| CHAPTER 6. SUMMARY AND CONCLUSIONS..... | 57 |
| 6.1 Introduction..... | 57 |
| 6.2 Applicability of RCMM..... | 58 |
| 6.3 Sensitivity of Hydraulic Modeling to Flow Rate and Bathymetry..... | 58 |
| 6.4 Comparison of Bathymetric Representations..... | 59 |
| 6.5 Future Work and Recommendations..... | 60 |
| LIST OF REFERENCES..... | 62 |

LIST OF TABLES

| Table | Page |
|--|------|
| 3.1 Description of study reaches..... | 18 |
| 3.2: Summary of the characteristic flows for the different reaches..... | 20 |
| 5.1: Summary of MAE with respect to the reference DEM for the different bathymetric configurations..... | 36 |
| 5.2: Performance statistics for inundation extent..... | 38 |
| 5.3: Summary of RE (%) for WSE..... | 39 |
| 5.4: Summary of RE (%) for flow area..... | 50 |
| 5.5: Summary of RE (%) for average velocity..... | 53 |
| 5.6: Summary of RE (%) for average shear..... | 54 |

LIST OF FIGURES

| Figure | Page |
|---|------|
| 3.1 Layout map of the study reaches..... | 13 |
| 3.2 Study reach of Strouds Creek..... | 14 |
| 3.3 Study reach of Tippecanoe River..... | 15 |
| 3.4 Study reach of St. Joseph River..... | 16 |
| 3.5 Study reach of East Fork White River..... | 17 |
| 3.6 Study reach of Brazos River..... | 18 |
| 3.7 Quantile-quantile plots showing fit for (a) Tippecanoe River, (b) St. Joseph River, (c) East Fork White River, and (d) Brazos River..... | 21 |
| 4.1 Difference between Linear1 and Linear2 model..... | 26 |
| 4.2 Flowchart showing the implementation of the RCMM1 and RCMM2..... | 28 |
| 5.1 Cross-section shape estimated for the five configurations for (a) Strouds Creek (Station Number 11716), (b) Tippecanoe River (Station Number 7534), (c) St. Joseph River (Station Number 26275), (d) East Fork White River (Station Number 36676), and (e) Brazos River (Station 65759)..... | 35 |
| 5.2 Comparison of flood maps for different bathymetric configurations of Tippecanoe River for (a) 10th percentile flow (F1); (b) 50th percentile flow (F3); and (c) 100-year flow (F6)..... | 40 |

| Figure | Page |
|--|------|
| 5.3 Comparison of flood maps for different bathymetric configurations of St. Joseph River for (a) 10th percentile flow (F1); (b) 50th percentile flow (F3); and (c) 100-year flow (F6)..... | 41 |
| 5.4 Comparison of flood maps for different bathymetric configurations of East Fork White River for (a) 10th percentile flow (F1); (b) 50th percentile flow (F3); and (c) 100-year flow (F6)..... | 42 |
| 5.5 Comparison of flood maps for different bathymetric configurations of Brazos River for (a) 10th percentile flow (F1); (b) 50th percentile flow (F3); and (c) 100-year flow (F6)..... | 43 |
| 5.6 Comparison of WSE for mean flow at (a) Tippecanoe River, (b) St. Joseph River, (c) East Fork White River, and (d) Brazos River..... | 48 |

LIST OF ABBREVIATIONS

| | |
|---------|---|
| 1D | One-dimensional |
| 2D | Two-dimensional |
| DEM | Digital Elevation Model |
| GIS | Geographic Information System |
| HEC-RAS | Hydrologic Engineering Center River Analysis System |
| LIDAR | Light Detection and Ranging |
| LP3 | Log-Pearson Type III probability distribution |
| MAE | Mean Absolute Error |
| NED | National Elevation Dataset |
| RE | Relative Error |
| RCMM | River Channel Morphology Model |
| SRTM | Shuttle Radar Topography Mission |
| USACE | United States Army Corps of Engineers |
| USGS | United States Geological Survey |
| WSE | Water Surface Elevations |

ABSTRACT

Dey, Sayan. M.S.C.E., Purdue University, August 2016. Role of River Bathymetry in Hydraulic Modeling of River Channel. Major Professor: Venkatesh Merwade.

Accurate geometric representation of the river channel is required for accurate hydraulic modeling of rivers. These are generally obtained through remote sensing techniques such as Light Detection and Ranging (LIDAR). However, these techniques lack the ability to model the submerged channel bed effectively and need to be complemented with surveyed bathymetric data for complete representation of the channel bathymetry, which can be time and cost prohibitive. An alternative to address this issue is to develop conceptual models that can estimate bathymetry.

This study aims to evaluate the potential of a conceptual model, the River Channel Morphology Model (RCMM) which estimates the channel bathymetry by relating channel planform to channel bathymetry. Channel DEMs are estimated from RCMM based algorithms and compared with those estimated from LIDAR and interpolation based algorithms to evaluate the importance and applicability of RCMM.

Each of the five channel DEMs is used to develop hydraulic models for three characteristic low and high flows. They are assessed to study the propagation of errors in channel DEM

to the hydraulic outputs such as inundation maps, water surface elevation (WSE), flow velocity and shear. The analysis shows that the error in hydraulic modeling due to inaccurate bathymetric representation is significantly reduced by RCMM. The error in hydraulic model outputs decreases with increasing flow.

The RCMM exhibits the ability to model channel bathymetry at reaches with reliable accuracy. Results indicate that the RCMM can even outperform bathymetry estimated from interpolation of surveyed data over large distances and, hence, is an admirable prospect for channel bathymetry estimation.

CHAPTER 1. INTRODUCTION

1.1 Background and Study Objective

Hydraulic modeling of rivers and streams is important for multiple applications ranging from estimating floods and assessing geomorphologic processes including sediment transport and riparian zone interactions, to ecological impact assessment which includes aquatic organism passage and fish habitat. Estimates of hydraulic variables such as inundation extent, water surface elevation (WSE) and flow velocity are critical parameters in these applications and can be easily estimated through hydraulic modeling of rivers.

However, the accuracy of these hydraulic models is significantly impacted by the uncertainty in the input datasets. The inputs to hydraulic models can be broadly classified into two categories: hydrologic inputs and topographic inputs (Bhuyian et al., 2015). Hydrologic inputs include flow and boundary conditions while the topographic inputs primarily provide information regarding the geometry of the river channel and floodplain.

The floodplain topography is often estimated by remote sensing techniques such as LIDAR. However, these techniques are unable to penetrate the water surface and, as such, do not provide any representation of the submerged channel bed. In order to reduce this uncertainty, they need to be complimented with bathymetric data. The channel bed is

traditionally estimated by determining the elevation at different points along the channel through field surveys such as total station based survey in the case of wadeable streams and boat mounted surveys in the case of deep rivers. The logistical constraints to such techniques often limit their application to reach scales only. Alternatively, remote sensing based methodologies have been developed to estimate bathymetry, but they are expensive and the uncertainty in their estimates increases with increasing depth and turbulence of the rivers (Gao, 2009; Legleiter & Overstreet, 2012; McKean et al., 2014).

Given the challenges of field surveys and remote sensing, conceptual models that can estimate bathymetry from easily available input parameters have become quite popular. These methods are inexpensive and can be implemented in large scale applications. Therefore any future approach should depend on the integration of observed bathymetry and conceptual models to create an accurate representation of river bathymetry. While several studies have proposed different algorithms to estimate river bathymetry, there is a need to quantify the effect of synthetic bathymetry on hydraulic models at different topographic settings and flow conditions.

This thesis explores the role of bathymetry incorporation in hydraulic simulation of river channels. The specific objectives of this study are as follows:

- 1) Compare different bathymetry creation techniques based on conceptual approach of River Channel Morphology Model (RCMM) and interpolation of cross-sections;
and

- 2) Assess the performance of high and low flow hydraulic simulations in response to different types of bathymetry inputs.

Besides providing insights into the role of bathymetry on hydraulic modeling of rivers, this study is expected to contribute to the emerging issue of increasing the accuracy of flow simulations on large scale river networks. As indicated earlier, both traditional field surveys and remote sensing techniques have limitations that restrict their application to individual reaches in a river network. A better understanding of different bathymetry generation methods can lead to large scale generation of river bathymetry, which can aid in improving the flow simulations in river networks.

1.2 Approach

In order to accomplish these objectives, bathymetric configurations are created using five different methodologies for five different study reaches in the U.S. namely the Strouds Creek (North Carolina), the Tippecanoe River (Indiana), the St. Joseph River (Indiana), the East Fork White River (Indiana) and the Brazos River (Texas). These reaches are located in different topographic settings and vary in reach length and size. Comparison of these bathymetric configurations across different rivers can help in determining the accuracy of these methodologies across multiple terrains and also help in evaluating the applicability of RCMM to different rivers.

Further, these study reaches are simulated for six flows: three high and three low flows. This is accomplished through 1D steady state modeling using the United States Army

Corps of Engineers' Hydrologic Engineering Center-River Analysis System (HEC-RAS: USACE, 2010). HEC-RAS provides estimates of hydraulic variables such as inundation extent, water surface elevation, flow velocity and average shear. Analysis of these hydraulic variables help in determining the applicability of the bathymetric models in the context of hydraulic modeling and evaluate the propagation of uncertainty in hydraulic modeling due to uncertain bathymetry.

Bathymetry estimated from all available surveyed data in a given reach is assumed to be the most accurate representation of channel bed. This configuration is therefore taken as reference. The performance of other bathymetric configurations are assessed by comparing the hydraulic outputs generated from them to those estimated from the reference model. To ensure consistency in comparison, all other parameters for hydraulic modeling are kept constant for the different bathymetric configurations of a given reach.

1.3 Thesis Organization

This thesis is organized in 6 chapters. The second chapter provides a review of the previous studies that aimed at estimating bathymetry and evaluating the effect of bathymetry on hydraulic modeling. The third chapter describes the study areas and other relevant details regarding input data. The fourth chapter outlines the procedure implemented in this thesis. It details the different methodologies used to estimate the bathymetry, and the modeling procedure used for estimating the hydraulic estimates. The results and discussions from these analyses are presented in chapter five. The sixth chapter summarizes the study and lists the conclusions of this study.

CHAPTER 2. LITERATURE REVIEW

2.1 Introduction

This study aims to evaluate the importance and applicability of RCMM in estimating river bathymetry. Section 2.2 reviews the existing techniques that are implemented for acquiring bathymetric data along with the studies to reduce the uncertainty associated with these techniques. Section 2.3 discusses the conceptual models that have been proposed in previous studies to estimate bathymetry in data-scarce regions.

2.2 Methods of acquiring bathymetry data

The techniques to measure bathymetry can be classified into two broad categories: field survey techniques and remote-sensing techniques. These are discussed in the following sections.

2.2.1 Field Survey Techniques

Traditionally, the point measurements of elevations are obtained through field survey techniques. These can either be land-based or boat-mounted. Land-based survey techniques such as total stations, terrestrial laser scanning or real-time kinematic global positioning system can be used to obtain bathymetry data at high resolution and precision (Feurer et al., 2008). Hilldale & Raff, (2008) noted that total station and real-time kinematic global

positioning system provide the best quality bathymetry data for shallow slow moving rivers.

Since these methods involve manual measurements, the surveyor's abilities have a significant effect on the accuracy of the observations (Bangen et al., 2014). The surveyor's safety considerations, especially in fast flowing or deep rivers, hinder the implementation of these surveying methods. Accessibility of river reaches and time constraints also affect the data density and accuracy (Jim McKean et al., 2009).

In relatively deep rivers, GPS-equipped boat-mounted surveying techniques which utilize echo sounders are more convenient (Hostache et al., 2015). Two popular examples are Acoustic Doppler current profiler (ADCP) and Sound Navigation and Ranging (SONAR) (Allouis et al., 2010). Echo sounders have been deployed using autonomous underwater vehicle (AUV) to collect bathymetry in marine estuaries (Wynn et al., 2014). These instruments provide point measurements of the elevation of river channel directly below the boat. These instruments have high precision and accuracy and can measure a large number of points. However, they need a minimum water depth that the boat can access, to be effectively employed and measurements are only taken along the path of the boat (Jim McKean et al., 2009). This leads to a reduction in the overall resolution of measurement, which can propagate error in estimating the topography. Other constraints include hindrances due to riparian vegetation, inability to measure steep sloping banks, and an inability to deploy for large-scale modeling due to high cost and intense labor (Allouis et al., 2010; Casas et al., 2006).

2.2.2 Remote Sensing

The logistical and safety challenges in field surveys have made remote-sensing an attractive alternative (Legleiter & Overstreet, 2012). These methods depend on satellite or aerial platform based electromagnetic sensors to measure the elevation and can survey large areas in a relatively small time (Casas et al., 2006). Topographic remote sensing has been widely used to characterize floodplains. However, topographic remote sensing often cannot penetrate the water surface, thus the bed topography (channel bathymetry) under the water surface is portrayed as a flat surface (Flener et al., 2012).

Various studies have implemented spectral photogrammetry to estimate the river bed characteristics. They take advantage of the fact that light backscatter decreases exponentially with increasing depth of the water column and therefore can be used to develop relationships between measured backscatter and water depth (Kinzel et al., 2013). These methods are only applicable in river depths ranging between 0.02m to 2m where visible light can penetrate the water and reach the channel bed and, hence, these methods need the river to be relatively clear in order to be accurate (Legleiter et al., 2015). Presence of vegetation in channel bed and algal cover also introduce uncertainty in bathymetry estimates (Feurer et al., 2008) which is especially relevant for Midwestern rivers.

In recent times, studies have explored the use of near infrared and green laser in order to develop bathymetric LIDAR surveys (Pan et al., 2015). They have a greater ability to penetrate the water surface as compared to traditional LIDARs. Like any other remote

sensing technique, the performance of bathymetric LIDAR also depends on the ability to penetrate the water and reach the channel bed.

A case in point is the Aquarius LIDAR which can penetrate and detect water column depths up to the order of 2 to 3m which reduces to around 1m for more turbid streams (Legleiter et al., 2015). Sediment particles and air bubbles act as point reflectors that can produce backscatter that do not correspond to the channel bed. This can introduce biases in the backscatter-depth relationships leading to errors in channel topography especially in shallow turbid streams (Kinzel et al., 2007; Legleiter et al., 2015; Pan et al., 2015).

An alternate method is to estimate the water surface from remote sensing and then solve an inverse hydraulic problem to estimate the channel geometry (Roux & Dartus, 2008). While the ease of acquiring data especially in inaccessible areas makes remote-sensing appealing, inability to acquire accurate estimates in murky, turbulent or deep streams and rivers pose major obstacles in these methods. Moreover, these methods have a high cost of implementation. For example, a LIDAR survey can cost \$1200 per square km (Bhuyian, Kalyanapu, & Nardi, 2015; Casas et al., 2006).

Several different algorithms have been proposed to reduce the uncertainties associated with representation of bathymetry in topographic datasets. Merwade et al. (2008) proposed GIS techniques for linear interpolation from surveyed cross-sections to compensate for the spacing between these cross-sections. Legleiter & Kyriakidis (2008) implemented a kriging based interpolation methodology to predict the cross-sections by adopting a simple

trend model and variograms. Both studies noted that the error in bathymetry is proportional to the cross-section spacing of the surveyed data.

Error propagation analyses of uncertain topography through a 2D hydrodynamic model have indicated that the uncertainty in outputs increases with decreasing topographic resolution and that the sensitivity of these outputs was found to be less for higher discharges (greater than 75% bank-full depth) as compared to lower discharges (Conner & Tonina, 2014; Cook & Merwade, 2009; Legleiter et al., 2011). However, such studies still need field survey data as inputs, the drawbacks of which have been highlighted before. Also, the need for relatively close spaced cross-section measurements limit their application to reach scales.

2.3 Conceptual models to estimate bathymetry

An entirely different approach to bathymetry estimation is the implementation of conceptual models that can estimate an approximate channel shape based on hydrodynamic or hydrologic variables. V. M. Merwade (2004) proposed the River Channel Morphology Model (RCMM) which modeled the spatial variability of a meandering river from the channel planform to estimate the bathymetry.

Price (2009) proposed a calibration technique to improve flood inundation mapping by assuming uniform cross-section over a river reach and progressively optimizing the channel parameters to create a functional surface. The parametric form of the bathymetry and the objective functions are based on the Saint-Venant equations in this study. Several

other studies have also proposed techniques to parametrize the cross-section and then calibrate the parameters using observed flows and depths to create synthetic cross-section shapes (Fread & Lewis, 1986; Garbrecht, 1990; Knight, 2006; Valiani & Caleffi, 2009). The main drawback of these methodologies is that they only produce a channel to improve flood routing and fail to account for the various physical processes that influence the channel planform.

Similarly, Bhuyian et al., (2015) proposed a DEM correction technique to improve flood routing by estimating the channel bed and subsequently, the thalweg from the side slope of the banks. Next, the channel depth and Manning's n are modified using an iterative process to estimate channel parameters. This methodology has the advantage of not using any data obtained from bathymetric surveys provided that stage-discharge data is available for the reach. Since the bathymetry estimates are solely dependent on the side slope, their accuracy is highly influenced by the quality of overbank slope estimates. Overbanks often contain vegetation, levees and other structures that hinder the accurate estimation of side slope which can further introduce significant errors in the model.

The appeal of the conceptual models lies in their ability to estimate bathymetry from easily accessible data such as channel planform and flow rate. This makes these models inexpensive and applicable in large scale application. Since the parameters of conceptual models are often derived from a particular reach, it is important to study the reliability of these models when they are applied to reaches with different topographic and landuse

settings. Often, a particular model performs well for a certain type of river but may be erroneous in other rivers.

2.4 Summary

In the context of large scale hydraulic modeling of rivers, accurate bathymetric representation plays a critical role. However, traditional field surveys are time and labor intensive, and limited to reach scale modeling only. On the other hand, remote sensing techniques have limited accuracy especially in deep, turbulent or turbid streams despite being very expensive. These challenges make conceptual models, such as RCMM, particularly appealing since they can produce bathymetric representations at reasonable accuracy for large scale applications without being data intensive. Therefore any future approach should depend on the integration of observed bathymetry and conceptual models to create river bathymetry. While several studies have proposed different algorithms to estimate the bathymetry, there is a need to quantify the effect of synthetic bathymetry on hydraulic models at different topographic setting and flow conditions.

CHAPTER 3. STUDY AREA AND DATA

3.1 Introduction

In order to test the reliability and accuracy of the bathymetric models, they need to be implemented and compared across a variety of river reaches and flow conditions. Therefore, the study sites comprise of five reaches of varying length, depth and geological settings in different parts of the U.S. Figure 3.1 shows the location of these reaches. These study reaches are described in the following section of this chapter. Table 3.1 summarizes the description of these reaches. Details regarding the datasets used in this study are then provided.

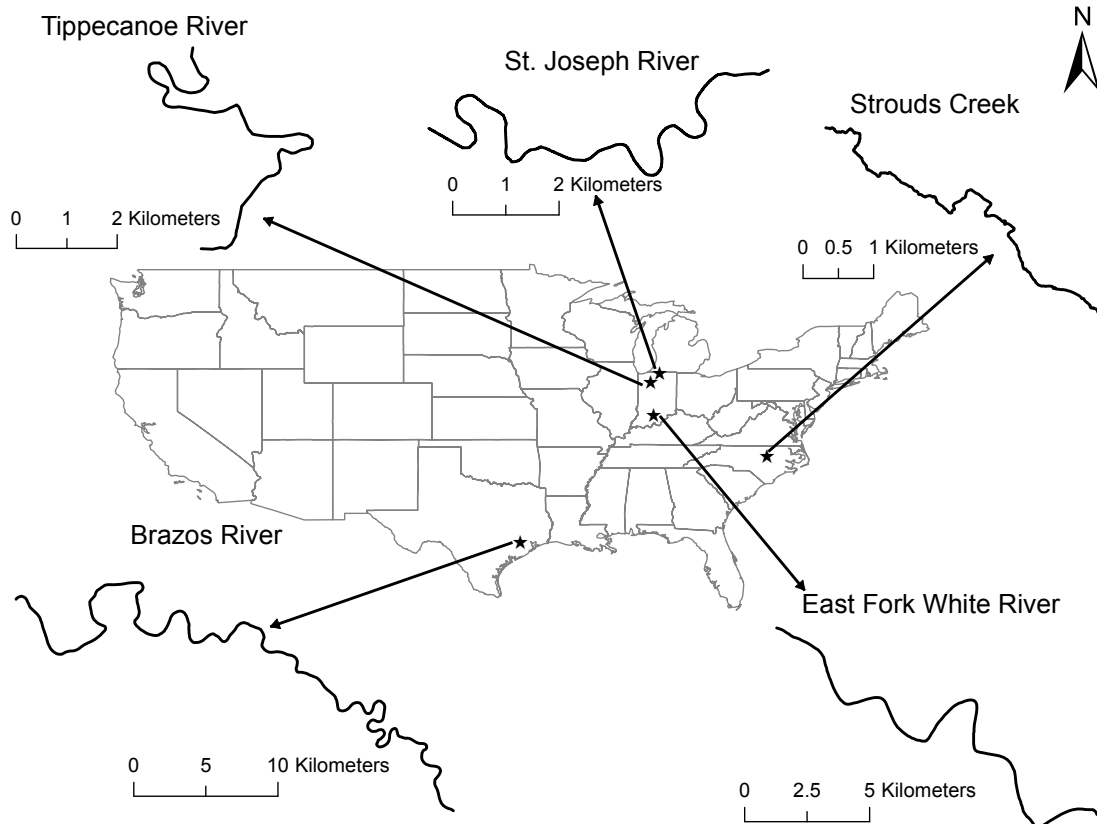


Figure 3.1: Layout map of the study reaches

3.2 Study Reaches

3.2.1 Strouds Creek

The Strouds Creek is located in Orange County, North Carolina. It meets the Eno River at the downstream end of the study reach. It is the shortest of the five reaches. It has a length of 6.5km and low sinuosity. It flows through a highly developed region. This stream is shallow and narrow with a primarily triangular shaped channel bed. It flows from north-west to south-east in this reach as shown in Figure 3.2.

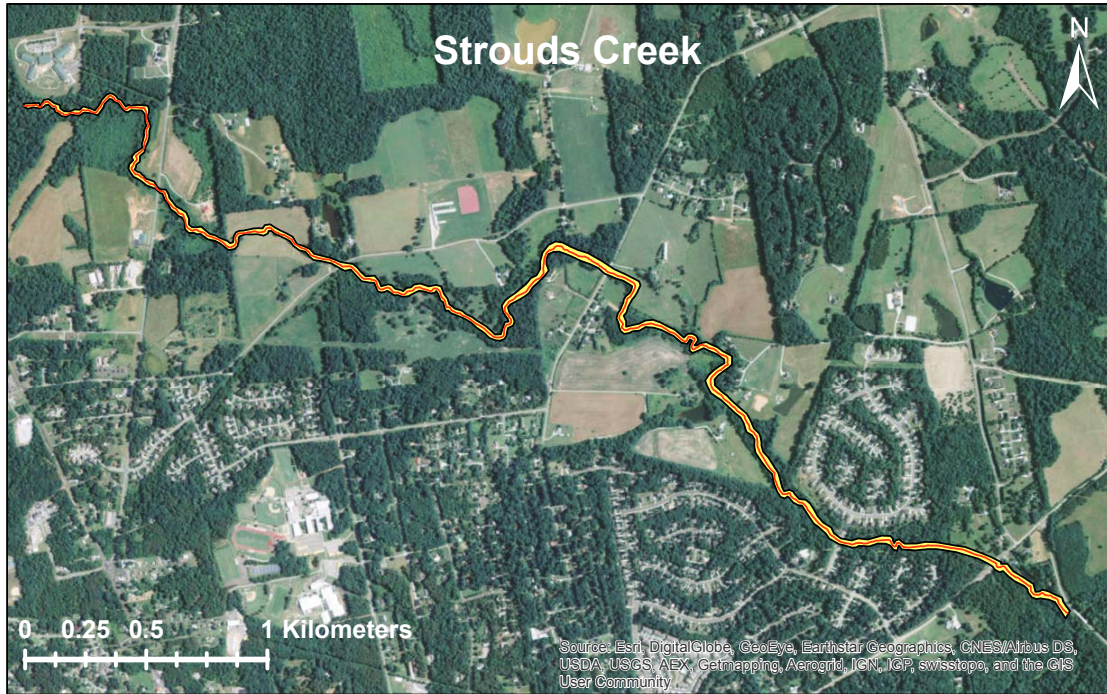


Figure 3.2: Study reach of Strouds Creek

3.2.2 Tippecanoe River

The Tippecanoe River reach is located near Winamac, in Pulaski County, Indiana. The 10.49km long reach has a narrow and shallow channel with an average bankfull depth of 2m. The channel is primarily V-shaped. This highly sinuous reach flows through an area dominated by urban landuse. It flows from north to south as shown in Figure 3.3. This reach is located in the middle portion of the Tippecanoe River where the channel bed is primarily sandy with some pea gravel (IDEM, 2001).

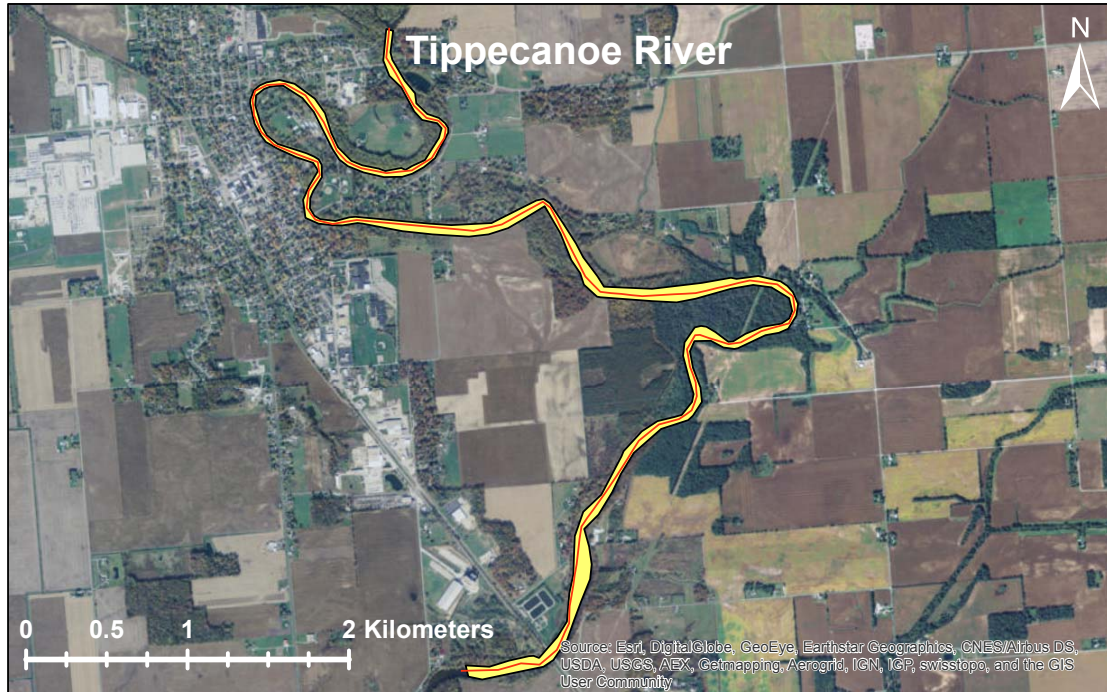


Figure 3.3: Study reach of Tippecanoe River

3.2.3 St. Joseph River

The third reach is St. Joseph River near Elkhart, Indiana. It is 11.18km long and the channel is primarily U-shaped. It flows from east to west as shown in Figure 3.4. It has a mean depth of 2.66m. Its channel width varies significantly along the reach. It is 50m wide at the upstream end and 408m wide at the downstream end. The reach flows through a developed region. This region is dominated by sand, silt and gravel which leads to high groundwater yield (Degraes, 2005).



Figure 3.4: Study reach of St. Joseph River

3.2.4 East Fork White River

The second longest reach is East Fork White River near Bedford, Indiana. It is a major tributary of the Wabash River. It is 20km long with a relatively deep channel and flat floodplains with few meanders. It has an urban setting with vegetation on both banks that serve as natural levees. It flows from south-east to north-west as shown in Figure 3.5. It is fairly uniform in width and has an average bankfull width of 80m and an average bankfull depth of 4m. The channel bed is primarily characterized by sand and silt with some gravel (Gray, 1989).

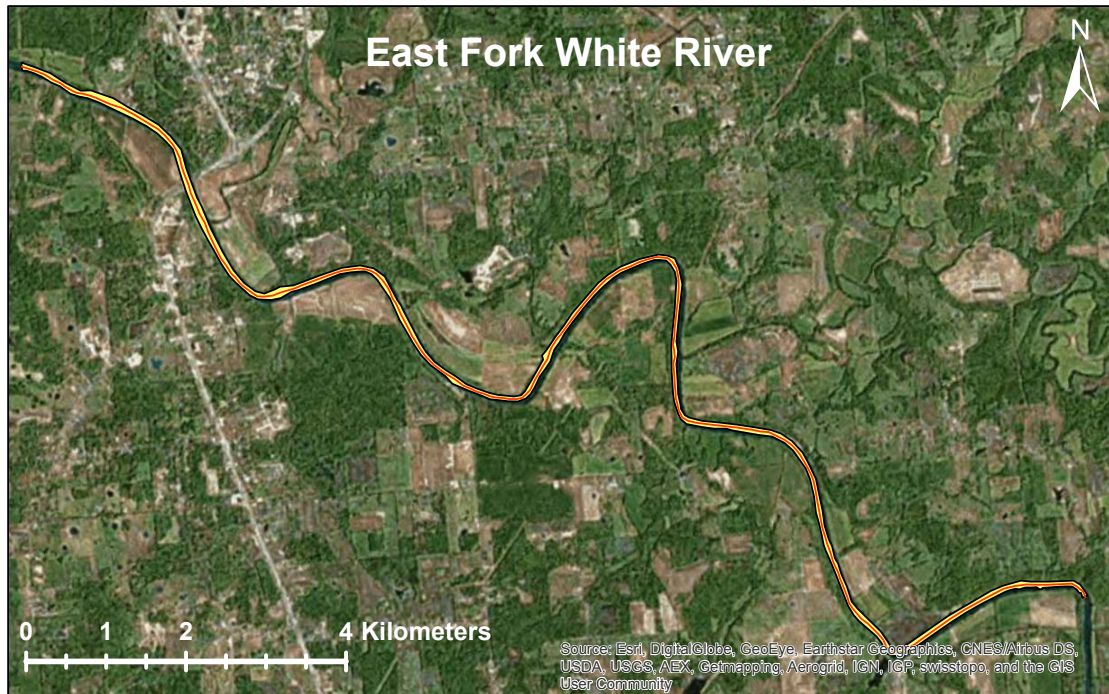


Figure 3.5: Study reach of East Fork White River

3.2.5 Brazos River

The Brazos River in Texas is the longest reach of the five with a length of approximately 60km. It is characterized by a relatively shallow, unbraided and silty channel with a number of meanders and a flat floodplain. The land-use is primarily agricultural. Because of recurring floods in the regions, levees have been constructed around the river channel. It flows from north-west to south-east direction as shown in Figure 3.6. It has a variable width ranging from 88m to 1011m and is approximately 13m deep.



Figure 3.6: Study reach of Brazos River

Table 3.1: Description of study reaches

| Reach | Reach Length (km) | Sinuosity |
|-----------------------|-------------------|-----------|
| Strouds Creek | 6.51 | 1.36 |
| Tippecanoe River | 10.49 | 2.63 |
| St. Joseph River | 11.18 | 1.73 |
| East Fork White River | 20.30 | 1.37 |
| Brazos River | 60.84 | 1.81 |

3.3 Flow Data

Since this study aims at analyzing the effect of bathymetry on both low and high flows, three characteristic low and high flows are selected. Some studies have denoted mean daily

flow as the upper boundary of low flows (Smakhtin, 2001). Hence, the three low flows adopted for this study are 10th percentile (F1), 25th percentile (F2) and 50th percentile (F3) daily flow. 10th percentile flow is used to characterize draught condition while 50th percentile flow is an indication of the central tendency of the flow distribution. High flows usually correspond to flood conditions. Therefore, flows greater than bank-full flows need to be selected. Bankfull flows correspond to flows with return period of 1 to 2 years (Robinson, 2013) and are considered to be channel maintaining flows. 100-year flow is often used as the design flow in designing of hydraulic structures. So flows corresponding to 2-year (F4), 10-year (F5) and 100-year (F6) return periods are chosen in this study.

Apart from Strouds Creek, each reach has a USGS streamflow gauge at the upstream end which is used to obtain the time series of annual maxima and daily mean flow. The streamflow time series is not available at Strouds Creek and the 100-year flow is obtained from Saksena & Merwade (2015).

The characteristic low flows are obtained by fitting a lognormal distribution (Beard, 1943) to the daily flow and estimating the 10 percentile, 25 percentile and 50 percentile flows. Figure 3.7 shows the quantile-quantile plot for the fitted lognormal distribution and the observed empirical distribution. It is evident from these plots that the fitted distribution follows the lognormal distribution reasonably. There are some deviations in the lower and upper tails but the fitted distribution models the observed distribution accurately in the 10th percentile to 50th percentile range, which is the range of flows (F1 – F3) used in this study.

For estimating the characteristic high flows, the procedure described in Bulletin 17b for obtaining flood frequency estimates (U.S. Water Resources Council, 1982) is implemented. The annual maxima time series obtained from USGS gauges is fitted with a Log-Pearson Type III (LPIII) distribution and the flows corresponding to return periods of 2 years, 10 years and 100 years (F4 – F6) are calculated.

The values corresponding to these six characteristic flows are tabulated in Table 3.2 for the study reaches used in this study.

Table 3.2: Summary of the characteristic flows for the different reaches

| Reach | Low Flow (m^3/s) | | | High Flows (m^3/s) | | |
|-----------------------|----------------------|----|----|------------------------|------|------|
| | F1 | F2 | F3 | F4 | F5 | F6 |
| Strouds Creek | - | - | - | - | - | 103 |
| Tippecanoe River | 8 | 12 | 21 | 130 | 217 | 325 |
| St. Joseph River | 43 | 59 | 84 | 277 | 425 | 605 |
| East Fork White River | 18 | 37 | 78 | 1107 | 1859 | 2361 |
| Brazos River | 17 | 38 | 94 | 1472 | 2702 | 3590 |

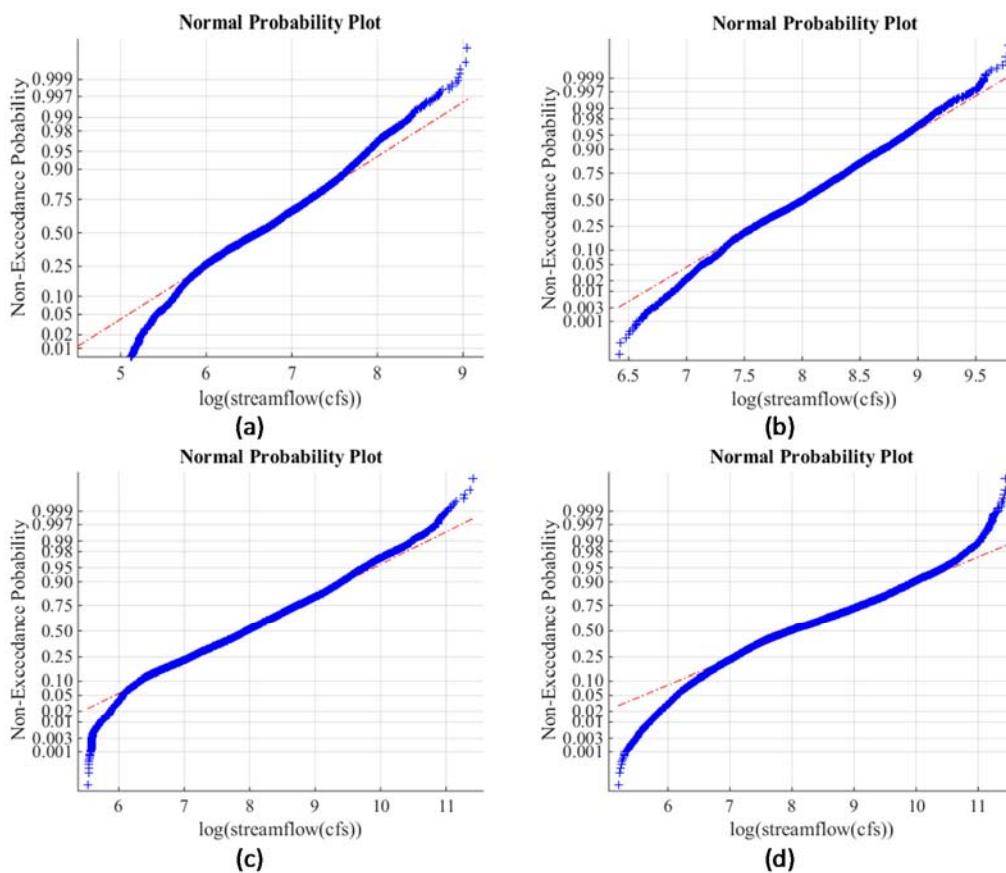


Figure 3.7: Quantile-quantile plots showing fit for (a) Tippecanoe River, (b) St. Joseph River, (c) East Fork White River, and (d) Brazos River.

3.4 LIDAR and Bathymetric Data

Bathymetry data are available in the form of point measurements obtained from boat-mounted echo sounders and a hand held GPS for all the study reaches except Strouds Creek. Bathymetry data for Strouds Creek was obtained using field surveyed cross-sections. Boat mounted echo sounder has a vertical accuracy of ± 1 cm.

Topography is represented in the form of LIDAR DEMs with a horizontal resolution of 3m (10ft). The vertical accuracy of LIDAR is reported to be 15cm – 25cm (Aguilar et al., 2010; Saksena & Merwade, 2015).

CHAPTER 4. METHODOLOGY

4.1 Introduction

To achieve the goal of evaluating the potential of RCMM as a conceptual model for estimating bathymetry, there is a need to implement it at different study reaches and compare its performance with bathymetric surfaces obtained from different methodologies. Assessing the hydraulic performance of channel bathymetry estimated using RCMM with other bathymetric surfaces can provide insights on the applicability of the RCMM in the context of hydraulic modeling.

The specific steps required to accomplish these goals are as follows: i) Development of 5 different bathymetric representations for each reach using different algorithms – 2 from conceptual models, 2 involving interpolation of surveyed cross-sections and one derived from topographic LIDAR based DEM; ii) Creation of integrated DEMs by incorporating channel bathymetry with surrounding floodplain topography; iii) Comparison of channel DEMs created in (i); and (iv) Comparison of hydraulic outputs estimated using the DEMs created in (ii). The following sub-sections discuss the 5 algorithms used in this study before elaborating on the methodology used for steps (ii), (iii) and (iv).

The subsequent sections in this chapter outline the algorithms using which the bathymetric models are derived and describe the procedures by which each of the above mentioned goals are established.

4.2 Description of Bathymetric Models

The first configuration incorporates all the surveyed cross-sections available for a reach to create a representative bathymetric surface. This is henceforth referred to as Linear1. The second configuration, Linear2, is created using only the most upstream and downstream surveyed cross-sections in a reach. This algorithm is similar to the methodology of (Gichamo et al., 2012; Saleh et al., 2012) which involves interpolating between the two cross-sections at the two ends of the reach. Gichamo (2011) proposed a conceptual model to estimate these two cross-sections whereas this approach uses the surveyed data for these two cross-sections.

The third configuration corresponds to the traditional RCMM, a conceptual model as described in Merwade, (2004), and is called RCMM1. It uses the channel boundary and the channel centerline to approximate the channel planform and does not incorporate any surveyed information. Often studies create synthetic channel planforms with idealized shapes such as trapezoid or parabola for developing cross-sections to approximate the river flow. A similar approach is included in this study in the form of RCMM2, the fourth configuration. It is based on a similar methodology as RCMM1 but creates a triangular shaped channel instead of fitting a beta distribution. Finally, the fifth configuration, LIDAR, does not use any bathymetric dataset and simply consists of a LiDAR based DEM.

4.2.1 Linear Interpolation (Linear1 and Linear2)

Bathymetric surveys provide point measurements of river channel but are sparsely spaced which can introduce errors when incorporated directly into a DEM. In order to circumvent this, the linear interpolation approach proposed in (Merwade et al., 2008) is adopted here. The point measurements are projected onto a line running across the channel to create a 3D cross-sectional representation of the river channel. Additional cross-sections are created between adjacent surveyed cross-sections by linearly interpolating the elevations of the points on these cross-sections.

Two bathymetric configurations, Linear1 and Linear2, are created using this approach. Linear1 incorporates all the available surveyed cross-sections to estimate the river planform. Since the surveyed cross-sections are situated fairly closely to each other in this study, Linear1 configuration is assumed to provide the best bathymetric representation. Therefore, hydraulic outputs estimated using Linear1 are taken as the reference for evaluating the performance of the rest of the bathymetric configurations.

Linear2 is created by linearly interpolating the channel planform between the most upstream and most downstream cross-sections, as illustrated in Figure 4.1. It provides a benchmark against which the RCMM models can be compared. Often, bathymetric data are available at streamflow gauges but not in the intermediate reaches. Bank elevation and thalweg depth can also be estimated at these gauged locations and used to implement the RCMM models. Comparison of the RCMM models with Linear2 model gives an idea about the performance of these models in such a situation.

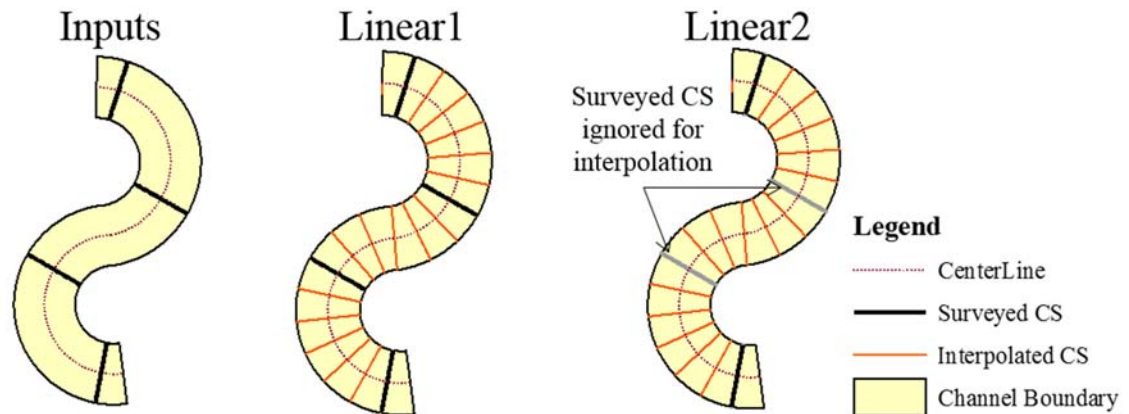


Figure 4.1: Difference between Linear1 and Linear2 model

4.2.2 RCMM (RCMM1 and RCMM2)

RCMM is a conceptual model that estimates the channel topography using channel planform information (Merwade, 2004). A meandering bend within a channel experiences sediment deposition on the inner bank and sediment erosion on the outer bank from the flowing water. This leads to an asymmetric channel cross-section with the thalweg being closer to the outer bank in a meander. At relatively straighter regions within the river, the thalweg roughly follows the centerline.

RCMM conceptualizes this physical process to create an empirical channel cross-section in three steps. In the first step, the channel shape is standardized into a non-dimensional space, where both the channel width and depth are equal to unity. In the second step, the thalweg is located by using the radius of curvature of the channel centerline through a power law function (Equation 1).

$$t^* = \begin{cases} a(r^*)^{-b} - 0.5, & r^* > 2 \\ 0, & r^* \leq 2 \end{cases} \quad (1)$$

where t^* is the thalweg location in normalized coordinate system where the width of the channel is unity, r^* is the normalized radius of curvature of the centerline segment, and a and b are parameters. The radius of curvature and the thalweg location are calculated for each meander in a 50km long reach in the Brazos River in Texas. The constants of Equation 1 are then estimated through least square regression.

In the third step, the three points defined by two bank locations and the thalweg are then used to generate a cross-sectional shape in the form of composite beta function using Equation 2. The parameters are estimated separately for different thalweg locations by least square regression of measured bathymetry data.

$$\widehat{z}^* = \{f(n^*|\alpha_1, \beta_1) + f(n^*|\alpha_2, \beta_2)\} \times k \quad (2)$$

where \widehat{z}^* is the depth estimate, $f(n^*|\alpha_1, \beta_1)$ and $f(n^*|\alpha_2, \beta_2)$ are the two beta functions and k , α_1 , β_1 , α_2 and β_2 are parameters that are dependent on the thalweg location.

In the final step, the normalized cross-section (width = 1 and thalweg depth = 1) is then rescaled using the bankfull width and depth at the corresponding cross-section. The bankfull width and depth for any cross-section along a reach are determined by linearly interpolating the input provided by the user at the upstream and downstream locations of the reach. The rescaled cross-sections can be joined to create a 3D mesh.

In this study, one other form of RCMM cross-section is created by simply joining the bank locations and the thalweg to give triangular cross-sections instead of composite beta functions. This is referred to as RCMM2. Figure 4.2 illustrates a flowchart for the algorithm of RCMM1 and RCMM2.

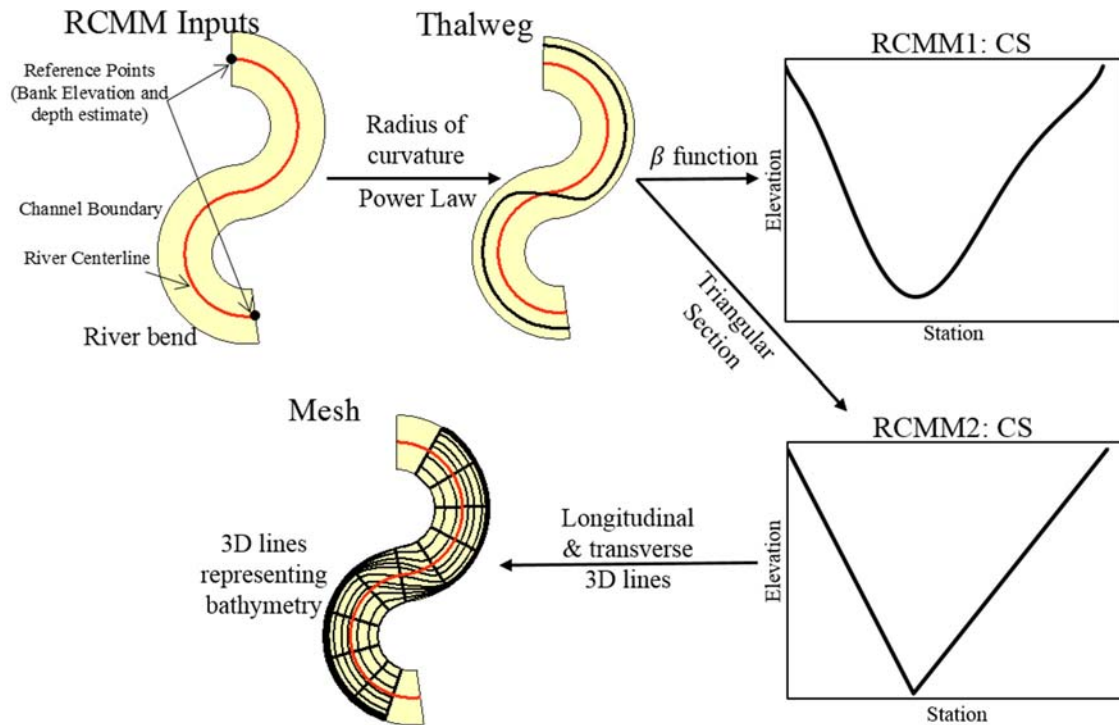


Figure 4.2: Flowchart showing the implementation and results of the RCMM1 and RCMM2

4.2.3 LIDAR

The final configuration involves the use of a DEM estimated from topographic LIDAR to estimate the geometry for hydraulic modeling without any bathymetry addition. Bathymetry has not been added to this DEM. As such, the channel below water (at the time of measurement) is depicted as a flat line; it's one-dimensional in the sense that it has width

but no depth. This model provides an estimate of the error that is propagated in a hydraulic model because of the error in bathymetry estimation by LIDAR, which in turn shows the extent of improvement due to bathymetry incorporation.

4.3 Bathymetry Integration

After creating the 3D mesh representations of the channel bathymetry using the models described above, they need to be incorporated into the DEMs for a complete representation of the topography. The 3D mesh is converted to points from which a DEM is created by interpolating between the points using natural neighbor technique.

The channel DEM is of the same resolution as the LiDAR DEM that is 3m (10ft). In case the mesh points were sparsely distributed along the channel, they were densified before creating the channel DEM using the densify tool in ArcGIS so that there is at least one point at every 3m spacing. The channel DEM is extracted using the channel boundary and then mosaicked with the LiDAR DEM to create the final DEM.

4.4 Hydraulic Modeling

The next step is to develop hydraulic models for each configuration. In this study, 1D HEC-RAS (Brunner, 2010) is adopted to perform the hydraulic modeling. HEC-RAS requires a geometric description of the channel in the form of the cross-sections for performing hydraulic computations. The number of cross-sections and the spacing between them varies from reach to reach depending upon the channel shape and reach length.

For a given reach, the cross-sections are located at the same locations for all 5 configurations in order to maintain consistency while evaluating the performance of the hydraulic modeling. Similarly, other HEC-RAS parameters, such as Manning's n and flow parameters, are also kept constant for different configurations of the same reach. The elevation corresponding to each point on the cross-sections is extracted from the bathymetry incorporated DEMs using HEC-GeoRAS (Ackerman, 2009). These are then imported into HEC-RAS to accomplish steady state 1D hydraulic modeling using the standard step energy method for six different flows. These flows have been discussed earlier and summarized in Table 3.2.

The simulations are run for the boundary condition that the water flows at normal depth at the most downstream cross-section. The flow along the reach is assumed to be constant and is equal to flow observed at the most upstream cross-section. Specifically for this study, the choice of the boundary condition is not relevant as long as it is the same for all configurations.

HEC-RAS provides estimates of hydraulic parameters such as flow depth, WSE and flow velocity at each cross-section which are imported into ArcGIS using HEC-GeoRAS. HEC-GeoRAS creates a raster of the hydraulic outputs such as WSE, velocity and shear by interpolating between the cross-sections. It subtracts WSE raster from the DEM raster to create a flow depth raster which can be used to estimate the flow depth and inundation extents corresponding to each flow.

4.5 Comparison of Bathymetric Configurations

The error in the topographic representation of different bathymetric configurations is evaluated using the mean absolute error (MAE) of the channel DEM as given in Equation 3.

$$MAE = \frac{\sum_{i=1}^n |E_m - E_r|}{n} \quad (3)$$

where E_m is the elevation of the i^{th} cell for the model being evaluated and E_r is the elevation of the i^{th} cell for the reference model which in this case is the Linear1 model, and n is the number of cells in the channel DEM. This gives an idea about which model is better estimating the channel topography.

Moreover, given the nonlinear nature of hydraulic modeling, it is also important to evaluate the extent to which these errors propagate to the hydraulic outputs. This is accomplished by assessing the inundation maps, channel velocity and shear. Accurate inundation maps are critical to flood-related applications. Velocity and shear are important parameters in hydraulic applications such as navigation and sediment transport. As such, comparing these hydraulic outputs help in determining the importance of these bathymetric representations for different hydraulic applications.

Accuracy of the inundation maps is determined by comparing the relative error (RE) in inundation area and average WSE for six flows. Additionally, the f -statistic is also calculated. These are depicted in Equations 4 and 5.

$$RE = \frac{X_m - X_r}{X_r} \times 100 \quad (4)$$

$$f = \frac{A_{op}}{A_o + A_p - A_{op}} \times 100 \quad (5)$$

where X_m is the estimate of hydraulic variable for a given model, X_r is the reference model estimate of a hydraulic variable, f is the f -statistic, A_o is the observed inundation area (inundation area of the reference model in this case), A_p is the modeled inundation area and A_{op} is the area that is common to both observed and modeled inundation maps. The relative error (RE) indicates the amount of overestimation or underestimation scaled with respect to the reference model. A negative RE shows underestimation whereas a positive RE indicates overestimation. The f -statistic assesses the accuracy of estimated inundated areas with respect to the reference model. A f -statistic of 100% corresponds to complete match between the observed and modeled inundation area which indicates that the model output is accurate. A f -statistic of 0% means that there is no overlap between the observed and predicted inundation areas. This points to poor model performance. Finally, the velocity and shear estimates of the various models for six flows are compared by calculating the RE with respect to the estimates obtained from the reference model.

CHAPTER 5. RESULTS AND DISCUSSION

5.1 Introduction

Five bathymetric DEMs are developed at six study reaches by implementing the methodology described in the previous section. Hydraulic modeling of these reaches produce estimates of hydraulic variables such as WSE, inundation area, flow velocity and shear. Results from the comparison of the channel DEMs and these hydraulic variables with the reference model (Linear1) are presented in this chapter along with a discussion on the performance of the various bathymetric models.

5.2 Comparison of DEM and Estimated Cross-sections

Figure 5.1 shows cross-sections estimated from the five different bathymetric configurations for the five study reaches. Except for Stroud's Creek, all four reaches show a flat line in case of LIDAR for the channel planform, which illustrates the inability of the LIDAR to penetrate the water surface and estimate the bathymetry. The Strouds Creek, despite being very shallow and narrow, suffers to a lesser extent from this problem but the LIDAR is still shallower when compared to the Linear1 model. These cross-section shapes give a qualitative idea about the reduction in flow area per cross-section in LIDAR when the cross-sectional geometry is extracted from LIDAR DEM.

For cross-sections estimated by the Linear2, the thalweg location can be quite erroneous when compared to Linear1. In some cases, such as that of Brazos River and Tippecanoe River, the thalweg is located on the other side of the center of the channel when compared to Linear1. The reason behind this discrepancy is the inability of Linear2 to model the spatial variability of the channel planform along a reach since Linear2 simply interpolates between two cross-sections located far from each other. It cannot account for the change in thalweg location and therefore, the determination of channel shape is erroneous. The error associated with Linear2 estimates is greater when the number of bends in the channel increases.

In the cases of Tippecanoe River, St. Joseph River and East Fork White River, the Linear2 model also fails to replicate even the general shape of the channel despite using two surveyed cross-sections as inputs. This shows the futility of interpolating over larger distances, especially in case of meandering rivers. In comparison, the thalweg of the RCMM1 and RCMM2 are located closer to that of Linear1. RCMM1 estimates reflect the channel shape as estimated by Linear1 but may underestimate or overestimate the cross-sections area.

Qualitatively, the RCMM1 and RCMM2 seem to perform the best among the four configurations being compared to Linear1. The difference between RCMM1 and RCMM2 estimates reduces for narrow and shallow reaches as is the case for Strouds Creek and Tippecanoe River but the difference between them increases as the channel becomes wider and deeper such as the Brazos River. The shape of the functional surface estimated by the

beta function (RCMM1) and triangular function (RCMM2) approximate each other when the scale of the reach is small which further reduces the differences between the channel cross-section elevations.

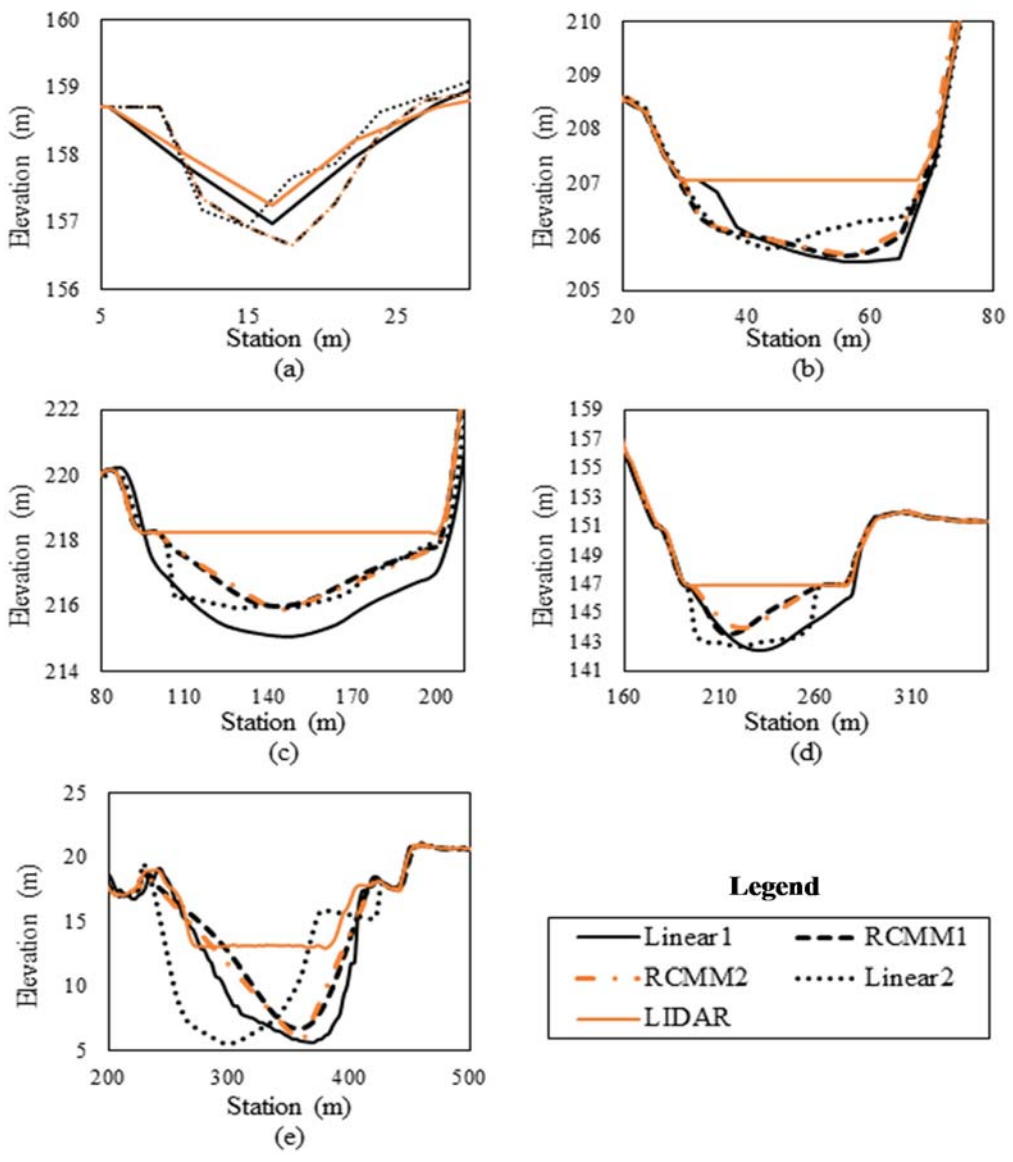


Figure 5.1: Cross-section shape estimated for the five configurations for (a) Strouds Creek (Station Number 11716), (b) Tippecanoe River (Station Number 7534), (c) St. Joseph River (Station Number 26275), (d) East Fork White River (Station Number 36676), and (e) Brazos River (Station 65759)

In order to carry out a more quantitative analysis, the MAE is tabulated for each site with respect to the Linear1 (reference model). These values are tabulated in Table 5.1.

Table 5.1: Summary of MAE with respect to the reference DEM (Linear1) for the different bathymetric configurations

| Reach | Topographic Model | | | |
|-----------------------|-------------------|-------|---------|-------|
| | RCMM1 | RCMM2 | Linear2 | LIDAR |
| Strouds Creek | 0.55 | 0.55 | 0.63 | 0.58 |
| Tippecanoe River | 0.60 | 0.61 | 0.62 | 1.00 |
| St. Joseph River | 1.27 | 1.28 | 1.47 | 2.09 |
| East Fork White River | 1.08 | 1.11 | 1.44 | 2.58 |
| Brazos River | 2.86 | 2.68 | 3.81 | 3.61 |

As shown in Table 5.1, LIDAR shows the maximum MAE for all reaches. It should be noted that the deepest part of the channel is denoted by a flat line in LIDAR and is the main contributor of MAE for LIDAR. This inability of LIDAR is particularly relevant in the context of hydraulic modeling since it can lead to underestimation of flow depth. The MAE of the other three configurations are significantly smaller than that of LIDAR indicating the importance of incorporating bathymetry for accurate representation of topography.

RCMM1 has the lowest MAE and is closely followed by RCMM2. This demonstrates the RCMM's ability to accurately estimate the bathymetry. The Linear2 also exhibits an improvement over LIDAR but is outperformed by the RCMM models. Despite the fact that Linear2 incorporates surveyed information which is harder to acquire, it is outperformed by RCMM models which makes a case for the RCMM models to be implemented for

bathymetry estimation especially in areas where surveyed cross-sections are unavailable or located at large distances. Among the five reaches, Strouds Creek has the lowest MAE followed by Tippecanoe River and East Fork White River. St. Joseph River has the second largest MAE, while Brazos has the largest MAE. This indicates that MAE is related to the bankfull depth and width; MAE increases with increasing bankfull depth and width. Since MAE is a scale-based performance statistic, this does not necessarily indicate that the configurations are more accurate at one site compared to another. Comparisons are only meaningful when different configurations are compared at the same site.

5.3 Comparison of Inundation Mapping

The analysis of channel DEMs show that the MAE is greatly reduced by the incorporation of bathymetry, but some uncertainty still remains for all bathymetric configurations. In order to study how this uncertainty propagates to hydraulic modeling, the DEMs with different bathymetric configurations are used to develop 1D hydraulic models for all the reaches for six flows.

As the flow increases, the inundation area and WSE are expected to increase. It is important to analyze how this variation is captured by the different topographic configurations for a given reach. Also, the five reaches behave differently at different flows owing to the variation in their channel and floodplain geometry. The inundation extent and WSE related performance statistic are tabulated in Tables 5.2 and 5.3 respectively.

Table 5.2: Performance statistics for inundation extent

| Reach | Flow | Reference Area (km^2) | RCMM1 | | RCMM2 | | Linear1 | | LIDAR | |
|-----------------------|------|---------------------------------|-----------|-----------------|-----------|-----------------|-----------|-----------------|-----------|-----------------|
| | | | RE (%) | <i>f</i> (%) | RE (%) | <i>f</i> (%) | RE (%) | <i>f</i> (%) | RE (%) | <i>f</i> (%) |
| Strouds Creek | F6 | 0.38 | 3 | 96 | 3 | 96 | 1 | 91 | 5 | 92 |
| Tippecanoe River | F1 | 0.49 | 24 | 70 | 24 | 70 | 21 | 68 | 44 | 60 |
| | F2 | 0.51 | 20 | 72 | 20 | 71 | 25 | 70 | 54 | 58 |
| | F3 | 0.58 | 11 | 79 | 10 | 78 | 18 | 78 | 63 | 57 |
| | F4 | 1.55 | -11 | 87 | -11 | 86 | 0 | 92 | 29 | 76 |
| | F5 | 2.05 | -6 | 93 | -6 | 92 | 0 | 97 | 11 | 89 |
| | F6 | 2.39 | -3 | 96 | -3 | 96 | 1 | 97 | 8 | 92 |
| St. Joseph River | F1 | 1.10 | -12 | 52 | -12 | 51 | -14 | 45 | 85 | 52 |
| | F2 | 1.21 | -11 | 56 | -11 | 55 | -16 | 49 | 74 | 56 |
| | F3 | 1.35 | -9 | 64 | -9 | 63 | -16 | 56 | 62 | 60 |
| | F4 | 1.90 | 7 | 85 | 6 | 86 | -2 | 85 | 53 | 64 |
| | F5 | 2.19 | 11 | 86 | 10 | 86 | 7 | 90 | 48 | 67 |
| | F6 | 2.54 | 10 | 89 | 10 | 89 | 8 | 90 | 42 | 70 |
| East Fork White River | F1 | 1.44 | -27 | 64 | -26 | 64 | 7 | 70 | 79 | 55 |
| | F2 | 1.53 | -13 | 73 | -13 | 73 | 5 | 74 | 97 | 50 |
| | F3 | 1.68 | 13 | 79 | 13 | 79 | -4 | 76 | 165 | 37 |
| | F4 | 13.80 | 6 | 94 | 6 | 94 | -10 | 90 | 13 | 88 |
| | F5 | 15.96 | 3 | 97 | 3 | 97 | -3 | 97 | 6 | 94 |
| | F6 | 16.79 | 2 | 98 | 2 | 98 | -2 | 98 | 5 | 95 |
| Brazos River | F1 | 4.05 | -25 | 34 | -38 | 33 | -10 | 26 | 72 | 43 |
| | F2 | 4.49 | -18 | 40 | -26 | 43 | -6 | 31 | 71 | 47 |
| | F3 | 5.09 | -10 | 48 | -10 | 53 | -4 | 37 | 72 | 48 |
| | F4 | 17.64 | 33 | 69 | 27 | 71 | -8 | 79 | 145 | 38 |
| | F5 | 41.65 | 52 | 57 | 35 | 62 | -15 | 79 | 195 | 33 |
| | F6 | 86.29 | 31 | 71 | 23 | 73 | -24 | 73 | 91 | 52 |

Table 5.3: Summary of RE (%) for WSE

| Reach | Flow | Reference WSE (<i>m</i>) | RE (%) Bathymetric Configuration | | | |
|--------------------------|------|----------------------------------|----------------------------------|-------|---------|-------|
| | | | RCMM1 | RCMM2 | Linear2 | LIDAR |
| Strouds Creek | F6 | 163.90 | 0.04 | 0.04 | 0.03 | 0.08 |
| Tippecanoe River | F1 | 206.30 | -0.12 | -0.11 | 0.20 | 0.45 |
| | F2 | 206.56 | -0.14 | -0.13 | 0.20 | 0.41 |
| | F3 | 206.93 | -0.16 | -0.15 | 0.19 | 0.35 |
| | F4 | 208.90 | -0.15 | -0.13 | 0.13 | 0.02 |
| | F5 | 209.62 | -0.11 | -0.09 | 0.11 | -0.03 |
| | F6 | 210.30 | -0.10 | -0.07 | 0.10 | -0.06 |
| St. Joseph River | F1 | 217.09 | 0.09 | 0.08 | -0.09 | 0.97 |
| | F2 | 217.28 | 0.11 | 0.10 | -0.06 | 0.97 |
| | F3 | 217.53 | 0.13 | 0.12 | -0.04 | 0.96 |
| | F4 | 218.80 | 0.16 | 0.15 | 0.06 | 0.87 |
| | F5 | 219.46 | 0.15 | 0.14 | 0.10 | 0.80 |
| | F6 | 220.06 | 0.15 | 0.14 | 0.10 | 0.75 |
| East Fork White River | F1 | 144.42 | 0.70 | 0.73 | -0.35 | 2.46 |
| | F2 | 144.84 | 0.89 | 0.91 | -0.32 | 2.44 |
| | F3 | 145.53 | 1.08 | 1.09 | -0.27 | 2.36 |
| | F4 | 151.15 | 0.43 | 0.43 | -0.11 | 0.85 |
| | F5 | 152.51 | 0.33 | 0.34 | -0.07 | 0.69 |
| | F6 | 153.21 | 0.31 | 0.32 | -0.07 | 0.66 |
| Brazos River | F1 | 9.86 | 1.51 | -3.71 | -10.59 | 49.07 |
| | F2 | 10.37 | 3.59 | -0.24 | -9.16 | 45.54 |
| | F3 | 11.24 | 6.17 | 3.59 | -7.28 | 40.47 |
| | F4 | 18.44 | 4.21 | 3.08 | -2.73 | 13.26 |
| | F5 | 20.66 | 2.03 | 1.26 | -2.13 | 7.14 |
| | F6 | 21.59 | 1.19 | 0.72 | -1.76 | 4.84 |

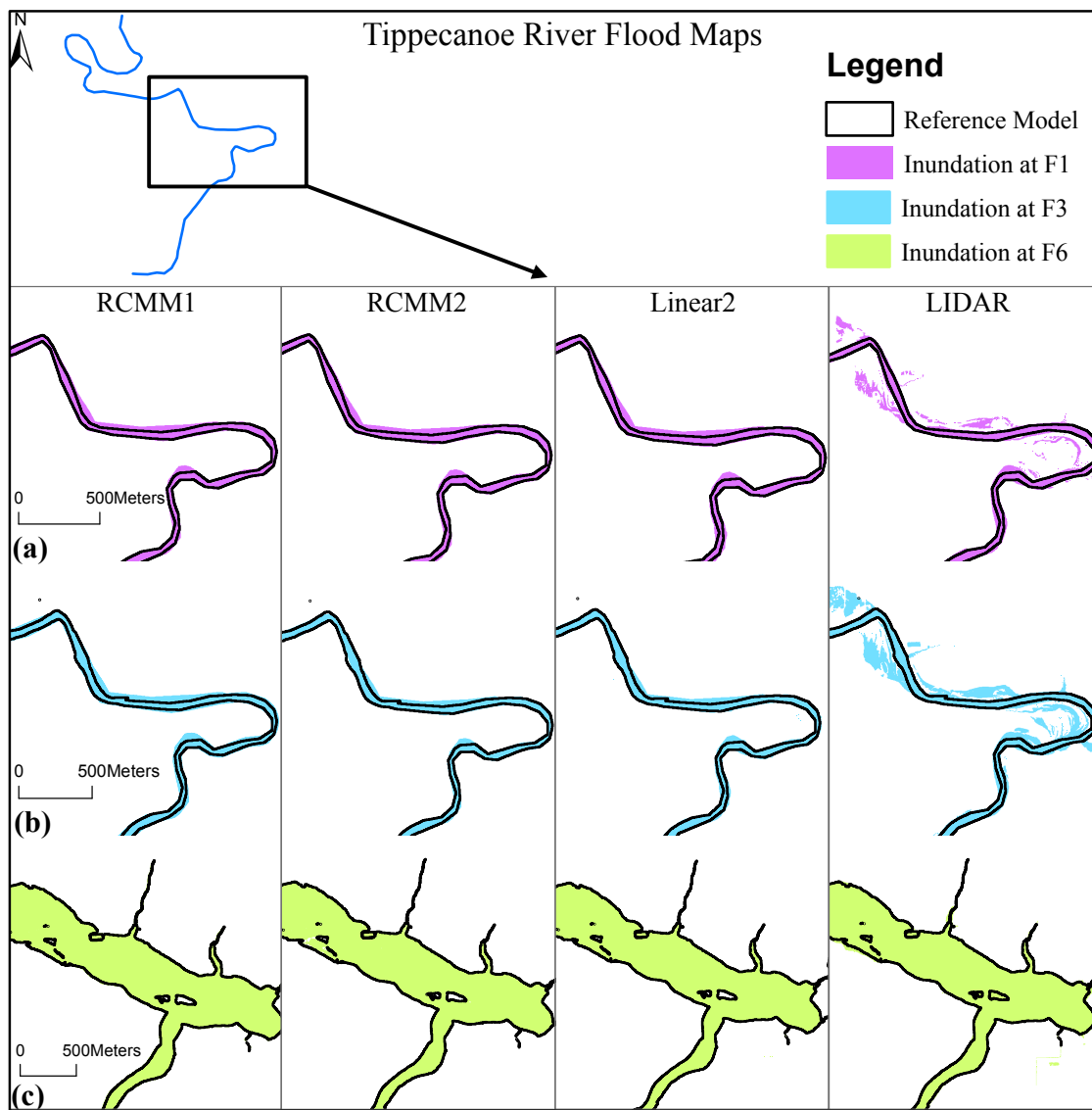


Figure 5.2: Comparison of flood maps for different bathymetric configurations of Tippecanoe River for (a) 10th percentile flow (F1); (b) 50th percentile flow (F3); and (c) 100-year flow (F6).

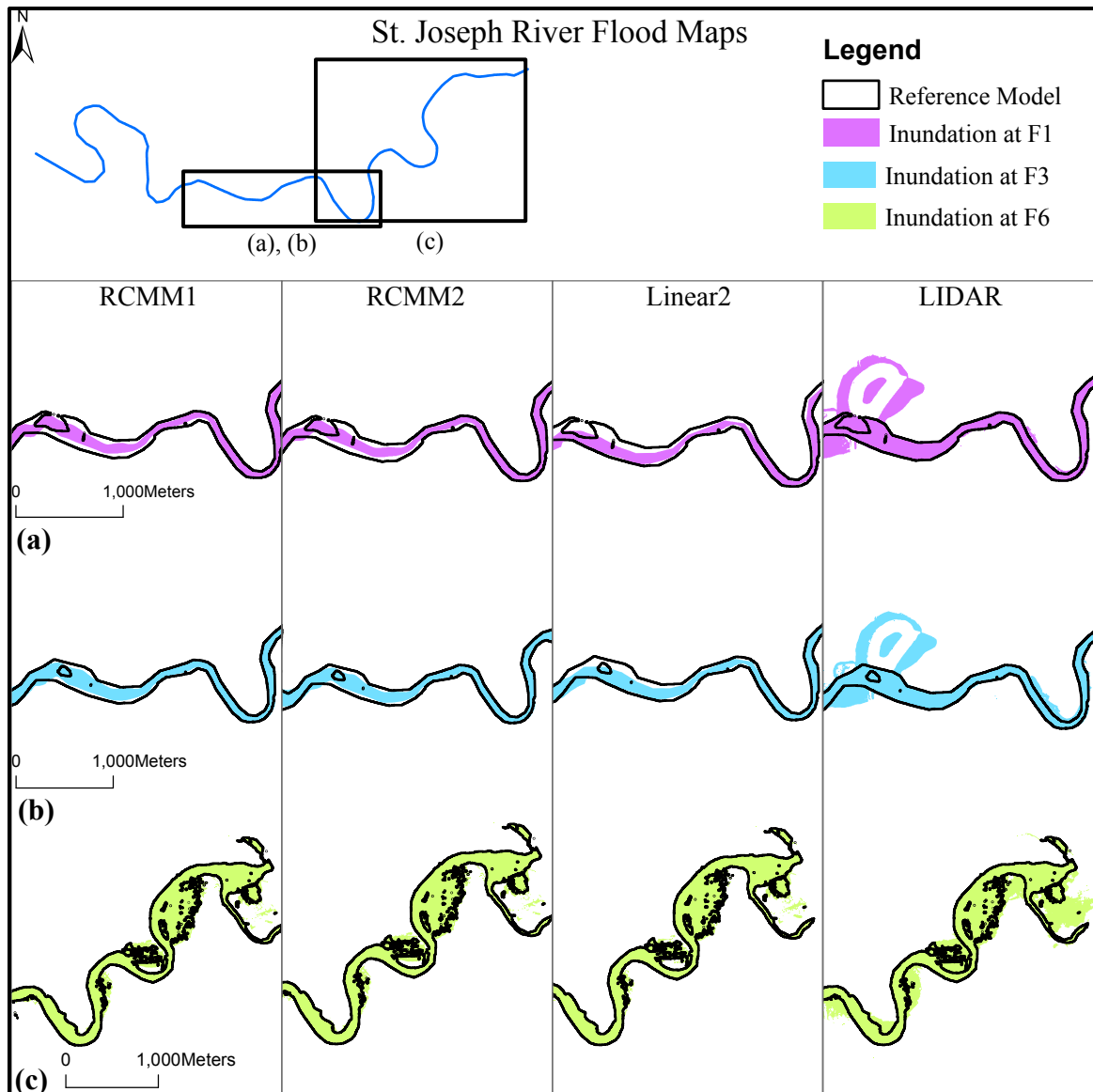


Figure 5.3: Comparison of flood maps for different bathymetric configurations of St. Joseph River for (a) 10th percentile flow (F1); (b) 50th percentile flow (F3); and (c) 100-year flow (F6).

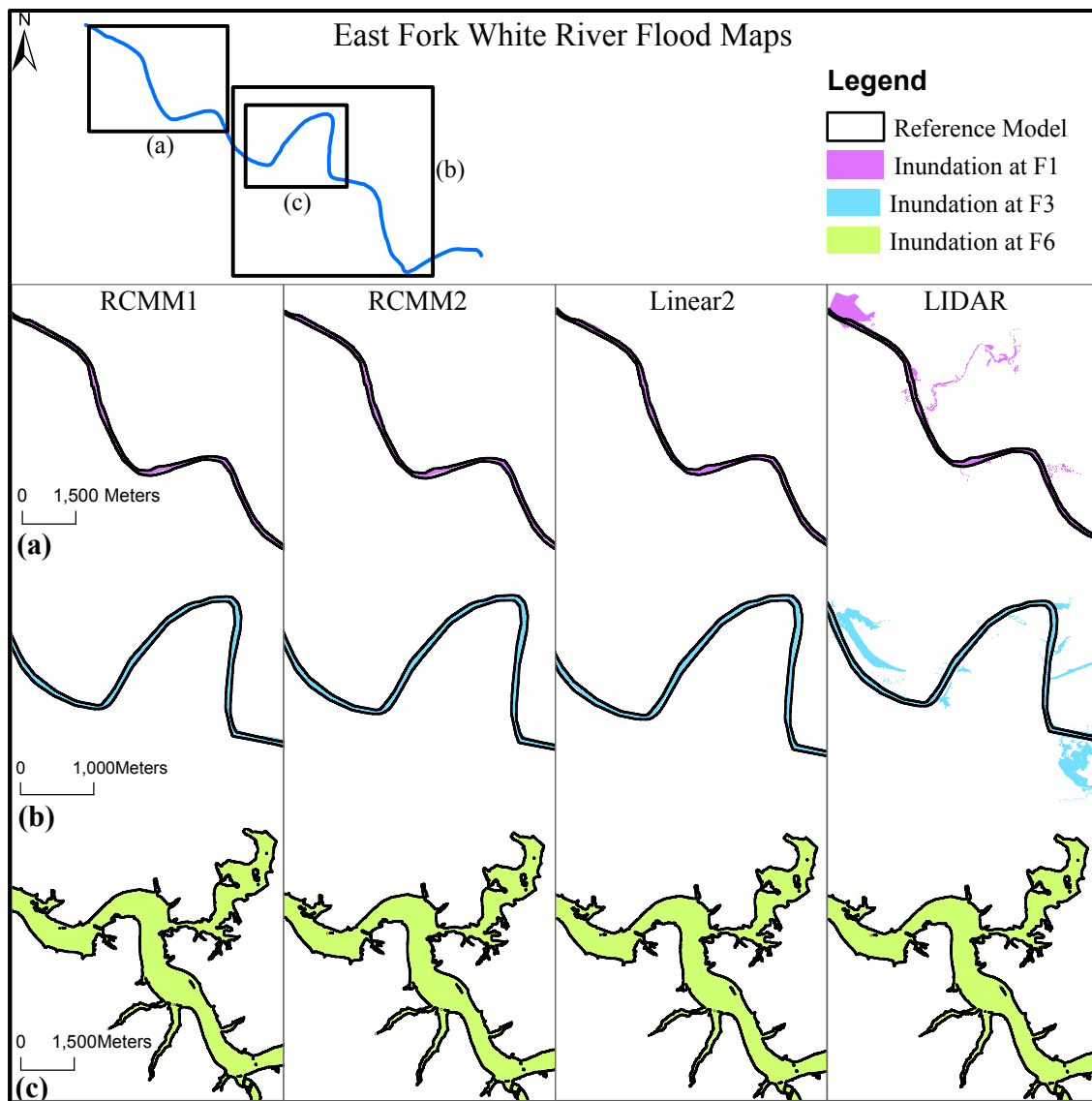


Figure 5.4: Comparison of flood maps for different bathymetric configurations of East Fork White River for (a) 10th percentile flow (F1); (b) 50th percentile flow (F3); and (c) 100-year flow (F6).

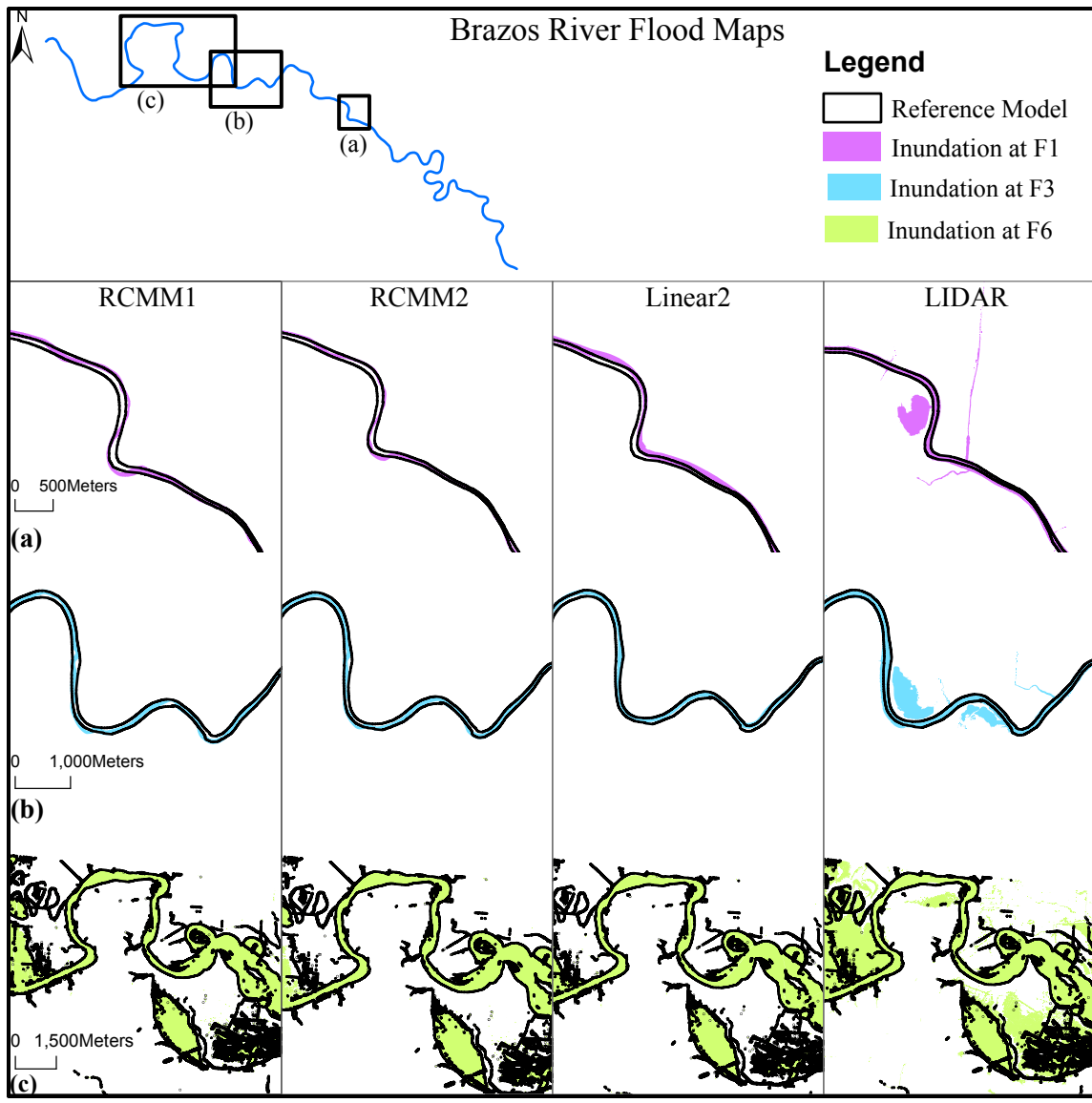


Figure 5.5: Comparison of flood maps for different bathymetric configurations of Brazos River for (a) 10th percentile flow (F1); (b) 50th percentile flow (F3); and (c) 100-year flow (F6).

The RE in WSE and inundation area is lower for the models that include bathymetry when compared to LIDAR for almost all the cases. The *f*-statistic is also the lowest for LIDAR. This result further reinforces the conclusions of Cook & Merwade, (2009) regarding the

improvement in hydraulic modeling when bathymetry is incorporated. The improvement is relatively small for shallow reaches such as the Strouds Creek and Tippecanoe River, but increases as the river becomes wider and deeper. For East Fork White River, the RE in inundation area reduces from 165% for LIDAR in case of F3 to just -4% in case of Linear2 and 13% in case RCMM1 and RCMM2. At Brazos River, the underestimation of channel storage by LIDAR can lead to significant errors in inundation area as illustrated by a RE of more than 70% for all flows. This overestimation is clearly demonstrated in the inundation maps for different reaches shown in Figures 5.2 – 5.5 for flows F1, F3 and F6. Even for F1, which corresponds to almost drought like conditions, LIDAR shows inundation outside the main channel for all the reaches, which is highly improbable.

Estimates of WSE and inundation area obtained from RCMM1, RCMM2 and Linear2 are closer to those of Linear1. The impact of bathymetry in estimating WSE is further illustrated in Figure 5.6. The estimates of WSE for F3 by LIDAR are much higher than that of the Linear1 (reference model). The errors are significantly reduced for RCMM1. The WSE estimates for RCMM1 follow the $y = x$ line more closely when compared to LIDAR for these four reaches. Additionally, this highlights the potential of RCMM1 in improving WSE estimates for different channel and topography characteristics.

The error associated with the models is higher at low flows. Both WSE and inundation area are highly sensitive to the bathymetry estimates at low flows. This is in line with the findings of Legleiter et al., (2011) who found that sensitivity to topographic uncertainty reduces for flows higher than 75% of bank-full flow. This can be attributed to the fact that

at low flows, the entire flow is confined to the main channel, and the topography of the river bed and geometry of the channel play a larger role in the velocity profile of the cross-section. The main channel is not captured accurately by LIDAR and but is replaced by river bathymetry estimates in the other models. For a given cross-section, the wetted perimeter is confined to the main channel for low flows. Thus, the hydraulic modeling is more sensitive to the bathymetry representation when the flows are conveyed inside the main channel. Moreover, the main channel is significantly narrower than the floodplain. A small change in flow condition will reasonably impact the WSE and inundation area. The floodplain, on the other hand, has the same elevations for all the bathymetric models for a given reach since it has been derived from the topographic DEM. The floodplain elevations are represented accurately by the topographic DEM. Therefore, as the flow increases and water inundates the floodplains, the impact of bathymetry incorporation reduces since the relative performance of all hydraulic models improves. The difference between the estimates from the different models also converge towards the reference model.

As the flow increases, the relative contribution of the water being routed in floodplains becomes more significant, and the effects of streambed topography reduces as the water depth increases. In case of F6, for a channel with small storage like Tippecanoe River, the water conveyed in the main channel is much smaller when compared to the floodplain leading to a very similar performance for all five models. Also, side-slopes of floodplains are less than those of the channel. Thus, even a small change in WSE leads to large change in flow and is accompanied by sharp change in inundation area. There is a stark increase between flow contained in the channel (flow less than bank-full discharge) and flow that

extends to the floodplains. This change is especially high for rivers with flat floodplains such as the East Fork White River and Brazos River.

The WSE and inundation area are moderately sensitive to magnitude of flow when low flow conditions exist. The f -statistic is highly sensitive at low flows but the sensitivity decreases with increasing flow. At high flows, a small increase in WSE can be accompanied by a large increase in inundation extent. So at low flows, f -statistic and WSE should be given priority for evaluating the model performance and flood inundation area should be of higher importance at high flows.

Among the topographic configurations that incorporate bathymetry, RCMM1 and RCMM2 have similar performance owing to similarity in cross-sectional shape as discussed earlier. The performance of Linear2 is better than RCMM in some cases whereas, in other cases, the RCMM models outperform Linear2. Since Linear2 interpolates between the most upstream and downstream surveyed cross-sections, its performance is dominated by the extent to which the bathymetry in the intermediate region is similar to these two cross-sections. Increase in spatial variation along the reach render it erroneous whereas the accuracy of Linear2 increases for reaches with less spatial variation. Since RCMM1 and RCMM2 model this spatial variability in the location of thalweg, they do not have uncharacteristically high errors in any of the cases. On the other hand, the performance of Linear2 can be highly varied as it can produce very accurate results for one flow and highly erroneous results at the other flows for the same reach. Therefore, RCMM1 and RCMM2 provide more reliable estimates of inundation maps when compared to Linear2.

Also, RCMM models the change in thalweg location along the reach, thus the inundation at low flows is better modeled by RCMM when compared to Linear2 which cannot account for the changing thalweg location. The flow conveyance in such cases tends to be one side of the channel for Linear2 which is highly inaccurate. Additionally, it is essential to note that Linear2 uses more surveyed data as inputs because it needs at least two completely surveyed cross-sections. The RCMM models only need depth estimates. In this context, the reliable performance of the RCMM models is admirable.

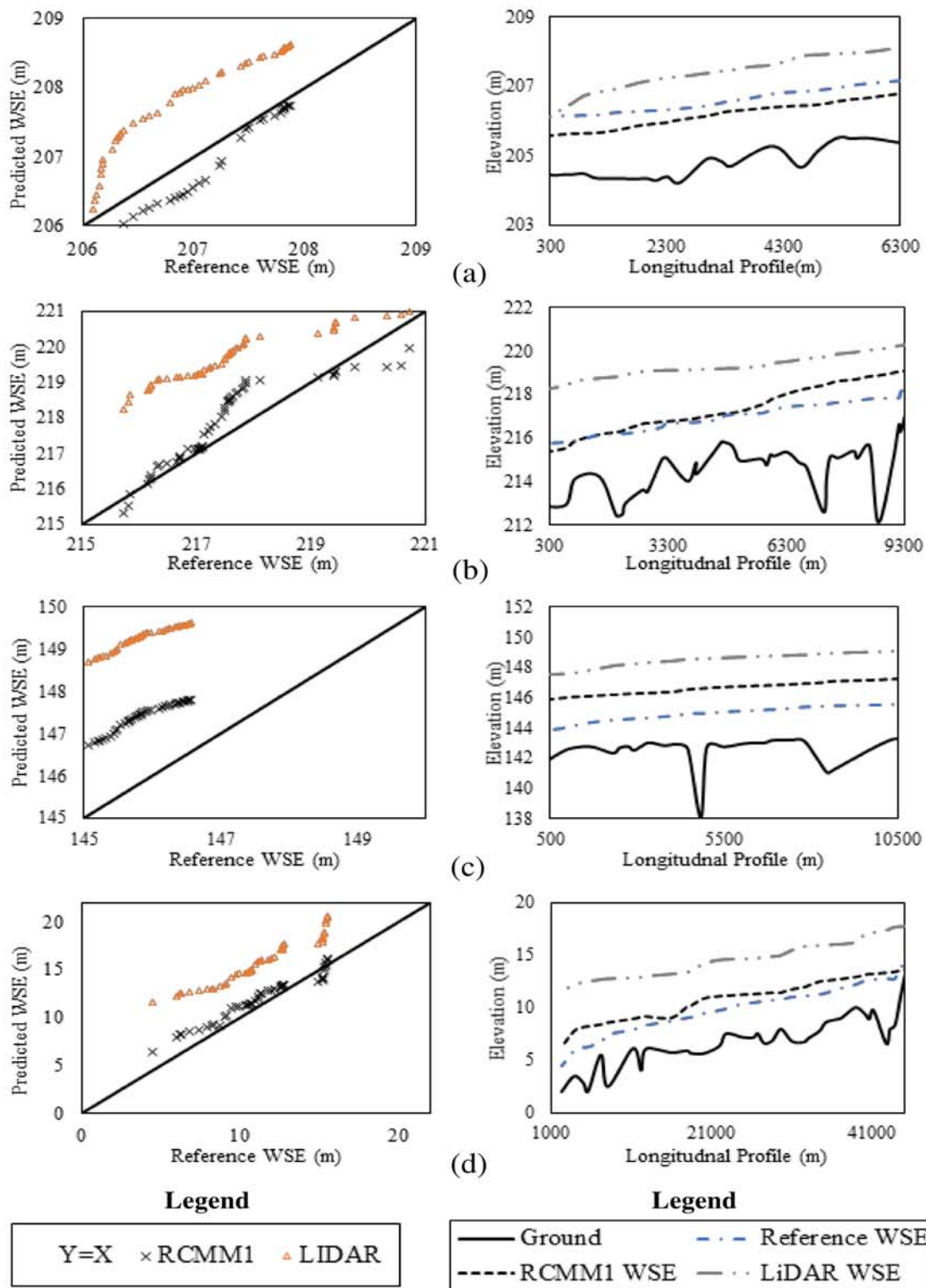


Figure 5.6: Comparison of WSE for mean flow at (a) Tippecanoe River, (b) St. Joseph River, (c) East Fork White River, and (d) Brazos River.

5.4 Comparison of Flow Areas at Cross-section

An important hydraulic variable in 1D hydraulic modeling is the flow area across a cross-section. It is related to the depth of flow and channel planform and affects the estimates of other hydraulic variables such as flow velocity. Inaccuracies in flow area estimates suggest the existence of errors in hydraulic modeling of rivers. In order to assess the flow area estimates of the bathymetric models in this study, the average flow area across all cross-sections are calculated and compared to the estimates obtained from Linear1. This comparison is tabulated in Table 5.4.

The flow area estimates obtained using all models shows improvement over LIDAR for all reaches except the Tippecanoe River. This can be attributed to the fact that the Tippecanoe River has a triangular channel accompanied with a V-shaped valley. The thalweg and WSE are both higher than those of the reference model. The increase in flow area in the floodplain is compensating for the loss of flow area in the channel in LIDAR leading to better flow area estimates. Essentially, the shape of the inundated area in the cross-section is different, as can be inferred from the difference in cross-section shapes shown in Figure 5.1, but the calculated area is the same.

Table 5.4: Summary of RE (%) for flow area

| Reach | Flow | Reference Flow Area (m^2) | RE (%) Bathymetric Configuration | | | |
|-----------------------|------|-------------------------------|----------------------------------|-------|---------|-------|
| | | | RCMM1 | RCMM2 | Linear2 | LIDAR |
| Strouds Creek | F6 | 72 | 4 | 4 | 4 | 6 |
| Tippecanoe River | F1 | 40 | -11 | -11 | 50 | -3 |
| | F2 | 53 | -9 | -9 | 41 | -1 |
| | F3 | 75 | -8 | -9 | 32 | 4 |
| | F4 | 361 | -18 | -19 | 17 | 3 |
| | F5 | 613 | -11 | -11 | 10 | -3 |
| | F6 | 893 | -8 | -8 | 7 | -5 |
| St. Joseph River | F1 | 119 | -27 | -28 | -30 | 35 |
| | F2 | 138 | -21 | -22 | -25 | 38 |
| | F3 | 166 | -17 | -17 | -19 | 39 |
| | F4 | 346 | -6 | -6 | -6 | 40 |
| | F5 | 466 | -2 | -2 | 3 | 39 |
| | F6 | 598 | 3 | 3 | 5 | 41 |
| East Fork White River | F1 | 79 | -17 | -17 | -12 | 46 |
| | F2 | 111 | -3 | -3 | -6 | 50 |
| | F3 | 166 | 12 | 12 | -1 | 67 |
| | F4 | 1669 | 25 | 26 | -5 | 50 |
| | F5 | 2874 | 13 | 13 | -3 | 27 |
| | F6 | 3573 | 11 | 11 | -2 | 22 |
| Brazos River | F1 | 144 | -50 | -56 | -54 | -25 |
| | F2 | 186 | -33 | -37 | -38 | -7 |
| | F3 | 267 | -14 | -13 | -21 | 15 |
| | F4 | 1724 | 18 | 17 | -6 | 40 |
| | F5 | 3058 | 17 | 13 | -7 | 63 |
| | F6 | 4467 | 4 | 14 | 4 | 52 |

In general, the estimates of flow area improve with increasing flow for all bathymetric configurations. As the flow increases, the main channel contributes less to the overall conveyance leading to a reduction in the impact of the incorporated bathymetry in hydraulic variables. The analysis of flow area indicates improvements in hydraulic modeling when bathymetry is included but flow area should not be used as the sole measure of improvement since two different wetted cross-section area shapes can yield same flow area. Other hydraulic variables such as flow velocity and average shear need to be analyzed to better assess the hydraulic performance of the bathymetric configurations.

5.5 Comparison of Velocity and Shear Estimates

RCMM1 and RCMM2 fit a functional surface to the river channel and therefore neglect the local variations in channel form such as riffles and pools. These local variations may impact the velocity of flow and the shear exerted on the river bed. This section analyzes the performance of the bathymetric configurations in terms of these two hydraulic variables by comparing the average flow velocity and the average shear exerted by the flow for different configurations. The average flow velocity estimates are tabulated in Table 5.5. Performance statistic related to shear are tabulated in Table 5.6.

It is interesting to note that for all reaches and at all flows, the RCMM1 and RCMM2 always give better estimates of velocity than the LIDAR. The same is also true for shear except for F1 (10 percentile) and F2 (25 percentile) flows at Brazos River. On the other hand, the performance of Linear2 is highly variable. It often provides estimates that are even poorer than the LIDAR estimates, but in some cases, it outperforms the RCMM

models and in other cases it remains somewhere in between. This shows that RCMM1 and RCMM2 are more robust options for hydraulic modeling in terms of velocity and shear estimates.

As mentioned earlier, the Linear2 cannot model the spatial variability of the channel bed especially at meanders. When the inundated area of the channel is dissimilar to the most upstream or downstream cross-section or the channel has high number of bends, the error associated with the Linear2 starts fluctuating which leads to a less reliable performance. The RCMM1 and RCMM2 aim at modeling the spatial variability in the channel bed, leading to more reliable performance across different flows. The performance of the RCMM models is even more impressive since they have significantly lesser data requirements for implementation. Therefore, in data sparse regions where surveyed cross-sections at high resolution are not available, the RCMM models should be given preference over interpolating over large distances in a reach.

As the flow rate increases, the associated velocity and shear should also increase. This effect is modeled by all the topographic representations for all reaches. The change in these estimates with respect to flow is considerable which shows that they are sensitive to both flow rate and topographic representation of the reach. In general, there is a significant difference or 'jump' in the relative error of these hydraulic variables between the 50 percentile flow and the 2-year flow which can be explained by the occurrence of bankfull discharge between these flows causes the water to inundate outside the main channel.

Table 5.5: Summary of RE (%) for average velocity

| Reach | Flow | Reference Shear (m/s) | RE (%) Bathymetric Configuration | | | |
|-----------------------|------|--------------------------|----------------------------------|--------|---------|--------|
| | | | RCMM1 | RCMM2 | Linear2 | LIDAR |
| Strouds Creek | F6 | 1.91 | -2.68 | -2.68 | -3.03 | -4.02 |
| Tippecanoe River | F1 | 0.23 | 1.12 | 1.52 | -16.23 | 4.46 |
| | F2 | 0.28 | 1.35 | 1.18 | -17.26 | 5.95 |
| | F3 | 0.34 | 3.25 | 3.18 | -19.41 | 9.87 |
| | F4 | 0.58 | 10.26 | 10.92 | -9.85 | 16.93 |
| | F5 | 0.65 | 7.74 | 8.07 | -6.17 | 19.79 |
| | F6 | 0.73 | 6.90 | 7.19 | -4.45 | 19.73 |
| St. Joseph River | F1 | 0.54 | 4.48 | 3.02 | 10.79 | -27.81 |
| | F2 | 0.59 | 4.80 | 3.63 | 11.45 | -24.52 |
| | F3 | 0.66 | 5.69 | 4.87 | 12.01 | -20.52 |
| | F4 | 1.00 | 5.19 | 4.83 | 9.81 | -12.02 |
| | F5 | 1.18 | 4.62 | 4.19 | 4.46 | -11.52 |
| | F6 | 1.36 | 3.41 | 2.90 | 2.65 | -12.70 |
| East Fork White River | F1 | 0.26 | 12.80 | 10.85 | 3.60 | -27.72 |
| | F2 | 0.35 | 1.21 | 0.02 | 1.07 | -23.89 |
| | F3 | 0.49 | -8.58 | -8.86 | -0.73 | -21.14 |
| | F4 | 1.38 | -10.64 | -10.69 | 0.78 | -23.40 |
| | F5 | 1.55 | -9.87 | -9.98 | 1.19 | -21.91 |
| | F6 | 1.63 | -9.44 | -9.57 | 1.13 | -20.94 |
| Brazos River | F1 | 0.32 | 4.83 | 8.26 | -6.40 | -23.26 |
| | F2 | 0.39 | 7.99 | 7.20 | -1.41 | -17.94 |
| | F3 | 0.53 | 1.70 | -0.04 | -1.49 | -24.51 |
| | F4 | 1.16 | -6.34 | -5.10 | 7.94 | -11.53 |
| | F5 | 1.38 | -6.09 | -4.27 | 6.67 | -12.89 |
| | F6 | 1.49 | -5.93 | -4.01 | 6.29 | -12.87 |

Table 5.6: Summary of RE (%) for average shear

| Reach | Flow | Reference Flow Area (N/m^2) | RE (%) Bathymetric Configuration | | | |
|--------------------------|------|---------------------------------------|----------------------------------|--------|---------|--------|
| | | | RCMM1 | RCMM2 | Linear2 | LIDAR |
| Strouds Creek | F6 | 7.63 | 1.55 | 1.55 | -2.12 | 6.95 |
| Tippecanoe River | F1 | 1.70 | -6.51 | -5.97 | 65.49 | 10.64 |
| | F2 | 2.08 | -1.17 | -0.94 | 23.21 | 12.05 |
| | F3 | 2.55 | 3.54 | 4.13 | -33.13 | 20.52 |
| | F4 | 2.97 | 25.82 | 26.44 | -19.24 | 118.76 |
| | F5 | 3.90 | 8.43 | 8.42 | -11.61 | 105.14 |
| | F6 | 4.87 | 7.89 | 7.19 | -8.52 | 67.95 |
| St. Joseph River | F1 | 6.96 | -27.91 | -30.29 | -18.39 | -68.52 |
| | F2 | 7.14 | -20.26 | -21.94 | -6.84 | -63.48 |
| | F3 | 7.54 | -12.21 | -14.29 | 2.56 | -57.26 |
| | F4 | 10.03 | -7.16 | -7.81 | 32.51 | -43.89 |
| | F5 | 10.75 | 0.51 | -0.51 | 8.31 | -35.13 |
| | F6 | 12.02 | 6.05 | 4.29 | 8.12 | -35.94 |
| East Fork White River | F1 | 1.03 | 12.40 | 0.00 | -5.79 | -57.17 |
| | F2 | 1.55 | -0.55 | -7.73 | -2.76 | -53.59 |
| | F3 | 2.53 | -26.69 | -30.07 | -2.36 | -53.72 |
| | F4 | 3.60 | 1.19 | 0.71 | 0.71 | 13.78 |
| | F5 | 5.18 | -0.33 | -0.50 | -3.80 | 5.78 |
| | F6 | 6.04 | -0.71 | -0.99 | -3.68 | 3.39 |
| Brazos River | F1 | 7.21 | -44.30 | -57.72 | -68.11 | -18.18 |
| | F2 | 8.14 | -34.40 | -50.90 | -57.80 | -10.61 |
| | F3 | 10.59 | -39.13 | -47.69 | -49.16 | -66.47 |
| | F4 | 13.65 | -19.91 | -17.85 | 21.74 | -45.77 |
| | F5 | 12.89 | -26.41 | -17.69 | 24.15 | -55.09 |
| | F6 | 9.50 | -22.02 | -13.80 | 44.36 | -36.47 |

The relative errors for velocity and shear estimates do not follow any specific trend with respect to flow. In some cases, the errors decrease and then increase with increasing flow whereas in other cases they increase and then decrease. Velocity estimates primarily depend on the flow area of the cross-section for a given flow rate (because of the continuity equation: $flow\ rate = area \times velocity$) while the wetted perimeter of a cross-section is one of the primary factors governing the estimation of shear in 1D hydraulic modeling. Significantly different cross-sections shapes may give nearly the same flow area or wetted perimeter for a certain flow, and can be erroneous at other flows. This effect propagates to the velocity and shear estimates leading to the absence of any specific trend. Also, at high flows, the channels behaves as a compound channel when the flow enters the floodplains which can increase the variability in the average values estimated for these variables. However, all the reaches exhibit significant errors for almost all flows when LIDAR model is used. Also, incorporation of bathymetry leads to considerable improvement for all flows barring a couple of exceptions, further highlighting the importance of bathymetry in hydraulic modeling.

In general, the velocity estimates of the hydraulic models are more accurate than the shear estimates. Not only do the velocity estimates have lower relative errors associated with different flows as compared to the shear estimates, the variation in relative errors is significantly lesser for velocity estimates. The velocity estimates depend on the accuracy of flow area estimates to an extent but do not strictly follow the trend shown by the flow area estimates. For the same magnitude of flow area produced by two different configurations corresponding to a given flow across a cross-section, the flow area in the

main channel and in the floodplains can differ. Since the main channel and floodplains have different Manning's n , flow velocity in the main channel and the floodplains will not be the same leading to different average velocity for that cross-section. The shear estimate depends on the wetted perimeter of a cross-section. When a smooth functional surface is fitted to the channel bed, the flow area is better captured by the model as compared to the wetted perimeter since the wetted perimeter is more sensitive to local variations and fluctuations. Therefore, the velocity estimates are more accurate as compared to the shear estimates.

CHAPTER 6. SUMMARY AND CONCLUSIONS

6.1 Introduction

Bathymetry is critical to the accuracy of hydraulic modeling of rivers. However, acquiring bathymetric data can be time- and labor-intensive especially for large scale hydraulic applications along with significant procurement costs. Therefore, there is a need for conceptual models that can estimate bathymetry in data sparse regions. This study aims at evaluating the applicability of RCMM, a conceptual model, to estimate bathymetry for hydraulic modeling of rivers. Three characteristic high and low flows are modeled at five different reaches with varying topography and channel characteristics.

The geometry of these reaches are represented by 5 different topographic configurations: (i) Linear1; (ii) RCMM1; (iii) RCMM2; (iv) Linear2; and (v) LIDAR. The Linear1 model incorporates all available surveyed cross-sections and is taken as the reference model. RCMM1 and RCMM2 are conceptual models used to estimate the bathymetry from the channel planform. Linear2 model interpolates the bathymetry using the most upstream and downstream surveyed cross-sections only. Comparison with LIDAR provides an indication of the error introduced by incomplete bathymetric representation. Evaluating the performance of RCMM1, RCMM2 and Linear2 with respect to the Linear1 model at

different study reaches quantify the relative applicability of conceptual bathymetric model in data sparse reaches in terms of improvement in hydraulic modeling.

6.2 Applicability of RCMM

The parameters of RCMM are estimated from the Brazos River reach. It is implemented in four other reaches with different channel characteristics in addition to Brazos River. The performance of RCMM1 and RCMM2 are analyzed by comparing the channel DEM and hydraulic variables (WSE, inundation area, flow velocity and shear) estimated from these two models to those estimated from Linear1. Low MAE and RE along with high f -statistic values indicate that the RCMM has the ability to estimate bathymetry for channels of varying topographic characteristics. The acceptable performance of these models at these reaches validates the fact that these model parameters are spatially transferable, that is, these can be implemented at other reaches.

6.3 Sensitivity of Hydraulic Modeling to Flow Rate and Bathymetry

Incomplete or inaccurate representation of bathymetry introduces significant error in the DEM which leads to erroneous hydraulic modeling of rivers. The error reduces significantly when bathymetry is incorporated in the DEM. In case of inundation mapping, for example, the error in a DEM with no additional bathymetry (LIDAR model) is as high as 85% in case of St. Joseph River at F1 and 195% for Brazos River reach at F5 which reduces to -12% for RCMM1 and -15% for Linear2 respectively.

The error associated with inundation maps and WSE reduce, in general, with increasing flow as demonstrated by an increasing f -statistic and decreasing relative error. For any given topographic dataset at any reach, the hydraulic modeling is most accurate at 100-year flow.

6.4 Comparison of Bathymetric Representations

The comparison of the channel DEMs produced by different bathymetric models with reference model indicate that the LIDAR DEM is highly erroneous in representing the main channel bathymetry. Topographic LIDAR fails to capture the river bed accurately which introduces significant errors in the DEM. Incorporating bathymetry significantly improves the channel DEM as characterized by considerable reduction in MAE. RCMM1 has the lowest MAE and is closely followed by RCMM2. Linear2 has a higher MAE when compared with RCMM1 and RCMM2 despite using surveyed cross-sections for estimating bathymetry.

The error introduced by interpolation over large distances is especially significant in case of meandering rivers. The thalweg location in the channel changes relative to its channel boundary as the river meanders. The Linear2 cannot account for this variation, which leads to fluctuations in its performance. RCMM1 and RCMM2 model this spatial variability and are, therefore, more reliable in bathymetry estimation. In most cases, greater the sinuosity of the river, more inaccurate the performance of Linear2 compared to the RCMM models.

RCMM models provide reliable estimates of flow velocity as compared to other bathymetric models as demonstrated by consistent improvement over the LIDAR estimates. In contrast, velocity estimates of Linear2 vary in accuracy and are often even worse than the LIDAR estimates.

Shear estimates fluctuate the most with respect to flow since shear is highly sensitive to local variations in cross-section shape. RCMM models cannot model these local variations leading to higher fluctuations in the model performance across different flows. However, the RCMM estimates are more accurate than those obtained from LIDAR, which further reinforces the applicability of RCMM in hydraulic modeling.

6.5 Future Work and Recommendations

This study demonstrates the importance of bathymetry in hydraulic modeling and the applicability of RCMM in estimating bathymetry in data sparse regions. RCMM is available for implementation as a toolbar in ArcGIS. As mentioned earlier, accurate estimation of bathymetry has applications in multiple domains including flood modeling, and evaluation of ecological impacts. Currently, the hydraulic fluxes or exchanges of water between the river channel and its floodplain are estimated using topographic LIDAR DEMs which do not contain information about the channel bed. By incorporating a functional bathymetric surface using RCMM, a better understanding of the river-floodplain hydrodynamics can be achieved. For large watersheds, the importance of bathymetry is more significant in estimating the channel beds of streams of lower stream order that contribute to a larger network of rivers. Therefore, bathymetry estimation has significant

implications on hydrologic estimation of large storm events over large watersheds. This study validates an approach to estimate bathymetry for single reaches. Future work involves developing a large watershed-scale approach of estimating bathymetry which would be useful in understanding not just hydraulic but also hydrologic processes. One of the future objectives is to develop a methodology for estimating bathymetry across river confluences which will help in extending RCMM to watershed scale.

The simulations carried out in this study are based on 1D steady-state hydraulic modeling at a fixed resolution. Further research in this direction should aim at evaluating the relative importance of bathymetry at coarser DEM resolutions. Also, 2D unsteady hydraulic models are expected to better represent the flow dynamics of the river especially for velocity and shear. Hence, the degree of improvement in such a model because of bathymetry incorporation need to be studied. Similarly, the results presented in this study are based on bathymetric estimation techniques for LIDAR-derived DEMs. While these DEMs do not contain river bathymetry, they do provide fairly accurate estimates of river floodplain. Future work also aims to expand RCMM application to DEMs derived from other sources such as the National Elevation Dataset (NED), which is available for the entire United States and the Shuttle Radar Topography Mission (SRTM), which is available globally but have higher uncertainty. If RCMM is developed to work at large scales and can be applied to estimate channel bathymetry using DEMs derived from multiple sources, the advantages can include significant improvements in model accuracy along with significant reduction in costs associated with field surveys.

LIST OF REFERENCES

LIST OF REFERENCES

- Aguilar, F. J., Mills, J. P., Delgado, J., Aguilar, M. A., Negreiros, J. G., & Pérez, J. L. (2010). Modelling vertical error in LiDAR-derived digital elevation models. *Journal of Photogrammetry and Remote Sensing*, 65(1), 103–110. <http://doi.org/10.1016/j.isprsjprs.2009.09.003>
- Allouis, T., Bailly, J., Pastol, Y., & Roux, C. Le. (2010). Comparison of LiDAR waveform processing methods for very shallow water bathymetry using Raman , near-infrared and green signals. *Earth Surface Processes and Landforms*, 35, 640–650. <http://doi.org/10.1002/esp.1959>
- Bangen, S. G., Wheaton, J. M., Bouwes, N., Bouwes, B., & Jordan, C. (2014). A methodological intercomparison of topographic survey techniques for characterizing wadeable streams and rivers. *Geomorphology*, 206, 343–361. <http://doi.org/10.1016/j.geomorph.2013.10.010>
- Bhuyian, N. M., Kalyanapu, A. J., & Nardi, F. (2015). Approach to Digital Elevation Model Correction by Improving Channel Conveyance. *Journal of Hydrologic Engineering*, 20(5), 1–10. [http://doi.org/10.1061/\(ASCE\)HE.1943-5584.0001020](http://doi.org/10.1061/(ASCE)HE.1943-5584.0001020).
- Brunner, G. (2010). *HEC-RAS, River Analysis System Hydraulic Reference Manual*.
- Casas, A., Benito, G., Thorndycraft, V. R., & Rico, M. (2006). The topographic data source of digital terrain models as a key element in the accuracy of hydraulic flood modelling. *Earth Surface Processes and Landforms*, 31(4), 444–456. <http://doi.org/10.1002/esp.1278>
- Conner, J. T., & Tonina, D. (2014). Effect of cross-section interpolated bathymetry on 2D hydrodynamic model results in a large river. *Earth Surface Processes and Landforms*, 39, 463–475. <http://doi.org/10.1002/esp.3458>

- Cook, A., & Merwade, V. (2009). Effect of topographic data , geometric configuration and modeling approach on flood inundation mapping. *Journal of Hydrology*, 377, 131–142. <http://doi.org/10.1016/j.jhydrol.2009.08.015>
- Degraves, A. (2005). *St. Joseph River Watershed Management Plan*. Friends of St. Joe River Association
- Feurer, D., Bailly, J.-S., Puech, C., Coarer, Y. Le, & Viau, A. A. (2008). Very-high-resolution mapping of river-immersed topography by remote sensing. *Progress in Physical Geography*, 32(4), 403–419. <http://doi.org/10.1177/0309133308096030>
- Flener, C., Lotsari, E., Alho, P., & Käyhkö, J. (2012). Comparison of empirical and theoretical remote sensing based bathymetry models in river environments. *River Research and Applications*, 133, 118–133. <http://doi.org/10.1002/rra.1441>
- Gao, J. (2009). Bathymetric mapping by means of remote sensing : methods , accuracy and limitations. *Progress in Physical Geography*, 33(1), 103–116. <http://doi.org/10.1177/0309133309105657>
- Gichamo, T. Z., Popescu, I., Jonoski, A., & Solomatine, D. (2012). River cross-section extraction from the ASTER global DEM for flood modeling. *Environmental Modelling and Software*, 31, 37–46. <http://doi.org/10.1016/j.envsoft.2011.12.003>
- Gray, H. H. (1989). Quaternary geologic map of Indiana: Bloomington, Ind., *Indiana Geological Survey Miscellaneous Map 49*.
- Hilldale, R. C., & Raff, D. (2008). Assessing the ability of airborne LiDAR to map river bathymetry. *Earth Surface Processes and Landforms*, 33, 773–783. <http://doi.org/10.1002/esp.1575>
- Hostache, R., Matgen, P., Giustarini, L., Teferle, F. N., Tailliez, C., Iffly, J., & Corato, G. (2015). A drifting GPS buoy for retrieving effective riverbed bathymetry. *Journal of Hydrology*, 520, 397–406. <http://doi.org/10.1016/j.jhydrol.2014.11.018>
- IDEM. (2001). *Tippecanoe River Watershed Restoration Action Strategy*. Indiana Department of Environmental Management , Office of Water Management.

- Kinzel, P. J., Legleiter, C. J., & Nelson, J. M. (2013). Mapping River Bathymetry with a Small Footprint Green LiDAR: Applications and Challenges. *Journal of the American Water Resources Association*, 49(1), 183–204.
<http://doi.org/10.1111/jawr.12008>
- Kinzel, P. J., Wright, C. W., Nelson, J. M., & Burman, A. R. (2007). Evaluation of an Experimental LiDAR for Surveying a Shallow, Braided, Sand-Bedded River. *Journal of Hydraulic Engineering*, 133(7), 838–842.
[http://doi.org/10.1061/\(ASCE\)0733-9429\(2007\)133:7\(838\)](http://doi.org/10.1061/(ASCE)0733-9429(2007)133:7(838))
- Legleiter, C. J., & Kyriakidis, P. C. (2008). Spatial prediction of river channel topography by kriging. *Earth Surface Processes and Landforms*, 33, 155–161.
<http://doi.org/10.1002/esp.1579>
- Legleiter, C. J., Kyriakidis, P. C., McDonald, R. R., & Nelson, J. M. (2011). Effects of uncertain topographic input data on two-dimensional flow modeling in a gravel-bed river. *Water Resources Research*, 47(3), 1–24.
<http://doi.org/10.1029/2010WR009618>
- Legleiter, C. J., & Overstreet, B. T. (2012). Mapping gravel bed river bathymetry from space. *Journal of Geophysical Research*, 117(F04024).
<http://doi.org/10.1029/2012JF002539>
- Legleiter, C. J., Overstreet, B. T., Glennie, C. L., Pan, Z., Fernandez-Diaz, J. C., & Singhania, A. (2015). Evaluating the capabilities of the CASI hyperspectral imaging system and Aquarius bathymetric LiDAR for measuring channel morphology in two distinct river environments. *Earth Surface Processes and Landforms*, 363(October 2015), 344–363. <http://doi.org/10.1002/esp.3794>
- McKean, J., Nagel, D., Tonina, D., Bailey, P., Wright, C. W., Bohn, C., & Nayegandhi, A. (2009). Remote Sensing of Channels and Riparian Zones with a Narrow-Beam Aquatic-Terrestrial LIDAR. *Remote Sensing*, (1), 1065–1096.
<http://doi.org/10.3390/rs1041065>
- McKean, J., Tonina, D., Bohn, C., & Wright, C. W. (2014). Effects of bathymetric lidar errors on flow properties predicted with a multi-dimensional hydraulic model. *Journal of Geophysical Research : Earth Surface*, 119, 644–664.
<http://doi.org/10.1002/2013JF002897>

- Merwade, V., Cook, A., & Coonrod, J. (2008). GIS techniques for creating river terrain models for hydrodynamic modeling and flood inundation mapping. *Environmental Modelling and Software*, 23(10-11), 1300–1311.
<http://doi.org/10.1016/j.envsoft.2008.03.005>
- Merwade, V. M. (2004). *Geospatial Description of River Channels in Three Dimensions*. The University of Texas at Austin.
- Pan, Z., Glennie, C., Hartzell, P., Fernandez-diaz, J. C., Legleiter, C., & Overstreet, B. (2015). Performance Assessment of High Resolution Airborne Full Waveform LiDAR for Shallow River Bathymetry. *Remote Sensing*, 7, 5133–5159.
<http://doi.org/10.3390/rs70505133>
- Price, R. K. (2009). An optimized routing model for flood forecasting. *Water Resources Research*, 45(2), 1–15. <http://doi.org/10.1029/2008WR007103>
- Robinson, B. A. (2013). *Regional Bankfull-Channel Dimensions of Non-Urban Wadeable Streams in Indiana*.
- Roux, H., & Dartus, D. (2008). Sensitivity Analysis and Predictive Uncertainty Using Inundation Observations for Parameter Estimation in Open-Channel Inverse Problem. *Journal of Hydraulic Engineering*, 134(5), 541–549.
[http://doi.org/10.1061/\(ASCE\)0733-9429\(2008\)134:5\(541\)](http://doi.org/10.1061/(ASCE)0733-9429(2008)134:5(541))
- Saksena, S., & Merwade, V. (2015). Incorporating the effect of DEM resolution and accuracy for improved flood inundation mapping. *Journal of Hydrology*, 530, 180–194. <http://doi.org/10.1016/j.jhydrol.2015.09.069>
- Saleh, F., Ducharne, A., Flipo, N., Oudin, L., & Ledoux, E. (2012). Impact of river bed morphology on discharge and water levels simulated by a 1D Saint – Venant hydraulic model at regional scale. *Journal of Hydrology*, 476, 1–9.
<http://doi.org/10.1016/j.jhydrol.2012.10.027>
- Smakhtin, V. U. (2001). Low flow hydrology : a review. *Journal of Hydrology*, (240), 147–186.
- U.S. Army Corps of Engineers. (2010). HEC-RAS River Analysis System. Hydraulic Reference Manual. Version 4.1. *Hydrologic Engineering Center (HEC), Davis, CA*, (January 2010), 411.

U.S. Water Resources Council. (1982). *Guidelines for Determining Flood Flow Frequency. Bulletin 17B: Guidelines for determining flood flow frequency.*

Wynn, R. B., Huvenne, V. A. I., Le Bas, T. P., Murton, B. J., Connelly, D. P., Bett, B. J., Ruhl, H. A., Morris K. J., Peakall J., Parsons, D. R., Sumner, E. J., Darby, S. E., Dorrell, R. M., Hunt, J. E. (2014). Autonomous Underwater Vehicles (AUVs): Their past, present and future contributions to the advancement of marine geoscience. *Marine Geology*, 352, 451–468. <http://doi.org/10.1016/j.margeo.2014.03.012>